bioactive proteins such as TNF-α improves their *in vivo* therapeutic potency [15,16]. However, protein PEGylation is mostly non-specific, targeting all of the lysine residues in a protein, some of which may be in, or near, an active site. As a result, PEGylation of proteins can result in substantial loss of specific activities. For example, PEGylated interferon (IFN)-α, which is a mixture of various positional isomers, has been used for the treatment of hepatitis C but has about 10% of the bioactivity of unmodified IFN-α [18]. Therefore, the clinical application of PEGylated proteins, with the exception of some bioactive proteins such as IFN-α, has been limited. Previously, we developed a novel strategy for site-specific mono-PEGylation, using TNF-α as a model, to improve *in vivo* anti-tumor potency and overcome the above-described limitations of PEGylation [19–21]. In addition, we created phage libraries that express mutant LTαs, in which the lysine residues of wild-type LTα (wtLTα) are substituted for other amino acids, and obtained mutants, including a TNFR1-selective mutant LTα [22].

Here, we attempted to create a lysine-deficient mutant LTα with bioactivity almost equivalent to that of wtLTα by using phage display. We also compared the value of site-specific PEGylation of lysine-deficient mutant LTα to that of random mono-PEGylation of wtLTα.

2. Materials and methods

2.1. Cells

LM cells, a mouse fibroblast cell line, were provided by Mochida Pharmaceutical Co. Ltd. (Tokyo, Japan) and maintained in MEM supplemented with 1% bovine fetal serum (FBS) and 1% antibiotics.

2.2. Construction of a library of lysine-deficient mutant LTαs

The phage library of lysine-deficient mutant LTαs was prepared as previously described [22]. Briefly, phagemid pY03′, encoding human wtLTα, in which the C-terminus of wtLTα is fused to the N-terminus of the M13 phage g3p, was used as a PCR template for constructing a DNA library of lysine-deficient mutant LTαs. Two-step PCR amplification was performed by using oligonucleotides containing the sequence NNS (which encodes all 20 standard amino acids) at Lys19, Lys28, Lys39, Lys84, Lys89, and Lys119 of wtLTα. The products from the second PCR were digested with NcoI and PstI and then ligated into pY03′. The phagemid was electroporated into *Escherichia coli* TG1 cells (Stratagene, Cedar Creek, TX), yielding 2×10^6 independent clones.

2.3. Selection of bioactive mutant LTα by using biopanning

An immunoplate was coated with 100 μL of soluble human TNFR1 (R&D Systems, Minneapolis, MN) at 10 μg/mL in 50 mM bicarbonate buffer (pH 9.5) and blocked with 10-fold diluted blocking buffer (Sigma–Aldrich, St. Louis, MO). A 100 μL volume of the prepared phage library was left to bind to each plate for 2 h at room temperature. After 10 rounds of washing with phosphate-buffered saline (PBS; pH 7.4) containing 0.05% Tween 20, and one final wash with PBS alone, bound phages were eluted with 150 μL of 10 mM glycine–HCl (pH 2.0) for 5 min at 4 °C. After neutralization with 75 μL of 1 M Tris–HCl (pH 8.0), the eluted phages were used to infect TG1 cells, which were then used for the second round of panning. After the second panning, single ampicillin-resistant colonies were picked and used to inoculate 500 μL of 2-YT medium containing 100 μg/mL of ampicillin and 2% glucose in deep 96-well plates. The plates were incubated in a shaker at 37 °C for several hours until the OD600 of the cultures reached approximately 0.5. We then added 10^8 plaque-forming units of M13KO7 helper phage to each well and incubated the plates for 30 min without shaking and for a further 30 min in a shaker at 37 °C. The cells in each well were pelleted by centrifugation and resuspended in 1 mL of 2-YT containing 100 μg/mL of ampicillin and 50 μg/mL of kanamycin. Cultures were incubated in a shaker at 25 °C for 6 h. The resulting phage-containing culture supernatant was used for screening by mixing with an equal volume of 5-fold diluted blocking buffer and then adding the sample to a TNFR1-immobilized ELISA plate. Bound receptor was detected by using a mouse anti-M13 antibody–horseradish peroxidase conjugate (GE Healthcare UK, Buckinghamshire, UK) and TMBZ (Wako Pure Chemical Industries, Japan). The DNA sequences of highly bound phage clones were obtained by using a ABI Prism 3100 (Applied Biosystems, Foster City, CA) and compared with that of the wtLTα-expressing phage.

2.4. Expression and purification of recombinant LTαs

pET15b plasmids (Novagen, Darmstadt, Germany) encoding LTαs were prepared and used to transform *E. coli* BL21(DE3) cells (Stratagene) for the expression of recombinant protein. Expression was induced by adding 1 mM isopropyl β-D-1-thiogalactopyranoside and incubating the cells at 37 °C for 6 h in Terrific Broth (Invitrogen Corporation, Carlsbad, CA) containing 0.4% glucose, 1.68 mM $MgSO_4$, and 100 μg/mL of ampicillin; all products were accumulated as inclusion bodies. Inclusion bodies prepared from cell lysates were washed in 25% Triton-X 100 and solubilized in 6 M guanidine-HCl, 100 mM Tris–HCl (pH 8.0), and 2 mM EDTA. Solubilized protein at 10 mg/mL was reduced with 10 mg/mL of dithioerythritol for 4 h at room temperature and refolded by 100-fold dilution in a refolding buffer (100 mM Tris–HCl, 2 mM EDTA, 1 M arginine, and 551 mg/L of oxidized glutathione); the buffer was adjusted to pH 8.5 with HCl. The LTαs were allowed to refold for 40 h at 4 °C. After dialysis against a buffer containing 20 mM Tris–HCl (pH 7.4) and 100 mM urea, active trimeric proteins were purified from the solution by using ion-exchange chromatography (SP Sepharose Fast Flow for wtLTα; Q Sepharose Fast Flow for LT-K0; both columns obtained from GE Healthcare). The eluates were further purified over a HiLoad Superdex 200PG column (GE Healthcare) equilibrated with PBS (pH 7.4).

2.5. Cytotoxicity assays

LM cells were seeded at 1×10^4 cells per well in 96-well plates and incubated at 37 °C for 72 h with serially diluted LTαs. After incubation, the cells were fixed by using glutaraldehyde and stained with 0.05% methylene blue for 15 min. After the cells were washed, 200 mL 0.33 N HCl was added to each well, and the absorbance of the released dye was measured at a wavelength of 655/415 nm.

2.6. PEGylation of LTαs

Activated methoxypolyethylene glycol succinimidyl propionate (PEG5K; molecular weight, 5000, Nektar, San Carlos, CA, USA) was used for PEGylation. wtLTα and LT-K0 in PBS were reacted with a 0.04-, 1-, and 25-fold (wtLTα) or 0.2-, 5-, and 125-fold (LT-K0) molar excess of PEG5 K (in terms of the total primary amine groups of LTα at 37 °C for 10 min. The reaction was stopped by adding ε-aminocaproic acid (10-times molar excess relative to the PEG5 K). The specific bioactivities of the mono-PEGylated forms of LTα were examined by using a cytotoxicity assay with LM cells. SDS-polyacylamidegel electrophoresis (SDS–PAGE) analysis of the PEGylated LTαs was conducted under reducing conditions, and the proteins in the gels were stained with Coomassie brilliant blue (CBB).

Table 1
Amino acid sequence of LT-K0, a lysine-deficient LTα mutant.

Residue position	19	28	39	84	89	119
wtLTα	Lys	Lys	Lys	Lys	Lys	Lys
LT-K0	Gln	Leu	Val	Pro	Gly	Ile

3. Results and discussion

3.1. Selection and production of the lysine-deficient LT-K0

Previously, to create fully bioactive lysine-deficient LTα mutants with all six lysine residues substituted, we constructed a phage library of LTα structural variants with randomized amino acids at the six lysine residues (Lys19, Lys28, Lys39, Lys84, Lys89, and Lys119) [22]. The constructed phage library yielded 2×10^6 independent clones (data not shown). To isolate the lysine-deficient LTα mutants that retained the bioactivity of wtLTα, we performed two rounds of affinity panning with human TNFR1 and the phage library. Potent binders to TNFR1 were concentrated in the library through this panning procedure. As a result, we obtained LT-K0, a putative lysine-deficient LTα mutant. DNA sequencing analysis of LT-K0 confirmed that all six of its lysine residues were mutated to other amino acids (Table 1). To investigate the properties of LT-K0 in detail, we prepared recombinant LT-K0 protein by using an *E. coli* expression system, as previously described. LT-K0 and wtLTα were expressed in *E. coli* and obtained through refolding of inclusion bodies. Purified LT-K0 and wtLTα had a molecular mass of 16 kDa by SDS–PAGE analysis (Fig. 1A) and approximately 50 kDa by gel filtration analysis (Fig. 1B), indicating that LT-K0 and wtLTα form homotrimeric complexes.

3.2. Bioactivity of the lysine-deficient mutant LT-K0

To assess the bioactivity of LT-K0, we performed cytotoxicity assays with LM cells, a clonal cell line sensitive to the pro-apoptotic effect of LTα (Fig. 2). wtLTα and LT-K0 showed dose-dependent cytotoxicity, and the bioactivity of LT-K0 was almost equal to that of wtLTα. These results suggest that LT-K0 is a lysine-deficient mutant LTα that retains the bioactivity of wtLTα,

3.3. Site-specific PEGylation of LT-K0

To confirm that LT-K0 is PEGylated specifically at the N-terminus, wtLTα and LT-K0 in PBS were reacted with a 0.04-, 1-, and 25-fold (wtLTα) or 0.2-, 5-, and 125-fold (LT-K0) molar excess of PEG5 K relative to their respective total primary amine groups.

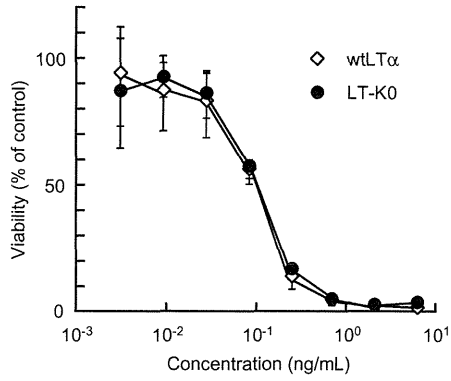

	EC50 (ng/mL)	Relative activity (%)
wtLTα	0.78	100.0
LT-K0	0.83	94.3

Fig. 2. Cytotoxic activity of wtLTα and LT-K0 against LM cells. *In vitro* murine TNFR1-mediated activity of wtLTα and LT-K0 against LM cells was measured by using a methylene blue assay. The EC50 is the concentration of LTα required for 50% inhibition of cell viability. Each value represents the mean ± S.D. ($n = 4$).

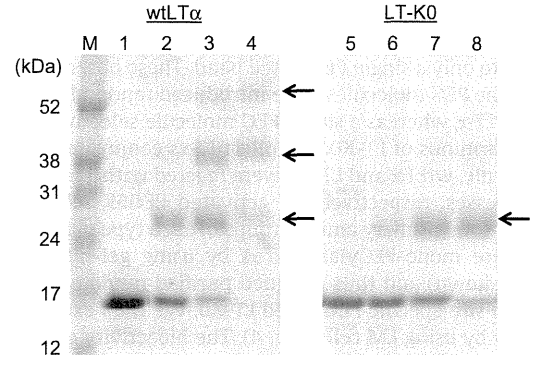

Fig. 3. SDS–PAGE analysis of PEGylated wtLTα and LT-K0. wtLTα and LT-K0 were reacted with activated PEG5K at molar excess amounts relative to the respective total primary amine groups of wtLTα and LT-K0. Lane M, molecular weight standards; lane 1, wtLTα; lanes 2–4, 0.04-, 1- and 25-fold molar excess of activated PEG5K relative to the total primary amine groups of wtLTα; lane 5, LT-K0; lanes 6–8, 0.2-, 5-, and 125-fold molar excess of activated PEG5K relative to the total primary amine groups of LT-K0. PEGylated LT-K0 was subjected to SDS–PAGE analysis and CBB staining.

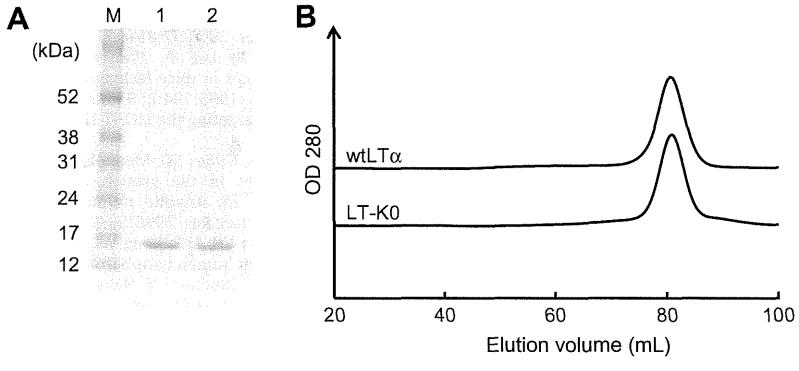

Fig. 1. Properties of recombinant LT-K0, a lysine-deficient LTα mutant. (A) SDS–PAGE analysis of wtLTα and LT-K0. All products were applied to SDS–PAGE gel and visualized by use of CBB staining. Lane M, molecular weight standards; lane 1, wtLTα; lane 2, LT-K0. (B) Gel-filtration analysis of purified wtLTα and LT-K0. wtLTα or LT-K0 was loaded onto a size-exclusion column and eluted at 1.0 mL/min.

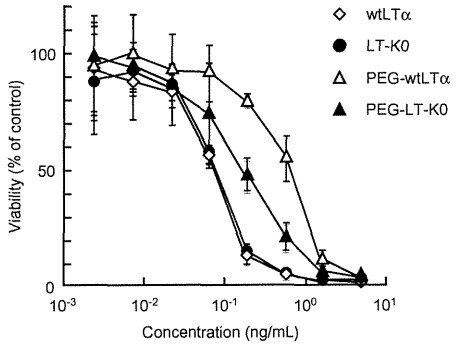

	EC50 (ng/mL)	Relative activity (%)
wtLTα	0.78	100.0
LT-K0	0.83	94.3
PEG-wtLTα	6.83	11.4
PEG-LT-K0	1.72	45.3

Fig. 4. Cytotoxic activity of PEGylated wtLTα and LT-K0 against LM cells. *In vitro* murine TNFR1-mediated activity of wtLTα and LT-K0 against LM cells was measured by using a methylene blue assay. The EC50 is the concentration of LTα required for 50% inhibition of cell viability. Each value represents the mean ± S.D. ($n = 4$).

PEGylated LTαs were detected by using SDS–PAGE followed by Coomassie brilliant blue staining. PEGylation of wtLTα resulted in multiple PEGylated bands (Fig. 3). In contrast, the PEGylation of LT-K0 led to only a single PEGylated band. These observations indicate that the PEG molecules were introduced randomly at multiple sites in wtLTα, whereas a single PEG molecule selectively attached to the N-terminus of LT-K0. To collect LTαs conjugated to a single PEG molecule, wtLTα and LT-K0 were reacted with 1- and 125-fold molar excesses, respectively, of activated PEG5K relative to the number of total primary amine groups of each type of LTα. We separated these mono-PEGylated LTαs by using gel-filtration HPLC (data not shown) and thus obtained purified randomly PEGylated wtLTα and site-specific PEGylated LT-K0. We then examined their bioactivity by using LM cells (Fig. 4). The bioactivity of wtLTα was decreased to 10% by random PEGylation. In contrast, although the bioactivity of LT-K0 was decreased to 50% by site-specific PEGylation, PEGylated LT-K0 retained five times the bioactivity of randomly PEGylated wtLTα. This site-specific mono-PEGylated LT-K0 thus retained the bioactivity that is generally lost following PEGylation, while maintaining the structural uniformity that is required of drugs.

Although conventional PEGylated drugs frequently have reduced activity as a result of PEGylation, this reduction is compensated for by an extended circulating lifetime in the blood, such that the PEGylated protein is more effective than the unmodified protein. When the circulating half-life of a drug is extended, passive targeting to tumor tissues is more probable via the EPR effect, which is due to the leaky nature of tumor blood vessels. Thus, PEGylated LT-K0 would be expected to show substantial anti-tumor efficacy in *in vivo* tumor models. In addition, it is known that LTα had equal antitumor activity in comparison to TNF-α but was less toxic [3]. Furthermore, we showed the *in vivo* dramatic antitumor effect by the site-specific PEGylated TNF-α [19]. These results suggest that PEGylated LT-K0 might be a superior candidate for cancer therapy, and we are now examining the usefulness of PEGylated LT-K0 *in vivo*.

Previously, we used a phage display technique to create a lysine-deficient mutant LTα, R1selLT, which had TNFR1-selective bioactivity [22]. In this study, we used LT-K0, the bioactivity of which was almost equal to that of wtLTα, to evaluate the utility of site-specific PEGylation *in vitro*. The next step will be to create site-specific PEGylated R1selLT and examine its therapeutic effect in tumor-bearing mice to evaluate the utility of site-specific PEGylation *in vivo*.

In this study, LT-K0 was conjugated to linear PEG5K, which is widely used for PEGylation of proteins. However, the molecular weight and shape of PEG strongly influence the *in vivo* stability of modified proteins [15,23]. In fact, *in vivo* stability increases with the molecular weight of PEG, whereas *in vitro* bioactivity decreases owing to steric hindrance [15]. Our group previously reported that optimization of the molecular weight and shape of PEG strongly improves anti-tumor activity [20]. Therefore, for maximum effectiveness of PEGylation, it is important to select the optimal molecular weight or type of PEG, balancing favorable effects, side effects, and dose schedules. We believe that such optimization will increase the usefulness of LT-K0.

Acknowledgments

The authors declare no conflict of interests. This study was supported in part by grants from the Ministry of Health, Labor, and Welfare of Japan; by a Research on Health Sciences Focusing on Drug Innovation grant from the Japan Health Sciences Foundation; and by the Takeda Science Foundation.

References

[1] Meltzer MS, Bartlett GL. Cytotoxicity in vitro by products of specifically stimulated spleen cells: susceptibility of tumor cells and normal cells. J. Natl. Cancer. Inst. 1972;49:1439–43.
[2] Beran M, Andersson BS, Kelleher P, Whalen K, McCredie K, Gutterman J. Diversity of the effect of recombinant tumor necrosis factors alpha and beta on human myelogenous leukemia cell lines. Blood 1987;69:721–6.
[3] Qin Z, van Tits LJ, Buurman WA, Blankenstein T. Human lymphotoxin has at least equal antitumor activity in comparison to human tumor necrosis factor but is less toxic in mice. Blood. 1995;85:2779–85.
[4] Paul NL, Ruddle NH. Lymphotoxin. Annu. Rev. Immunol. 1988;6:407–38.
[5] Cuff CA, Schwartz J, Bergman CM, Russell KS, Bender JR, Ruddle NH. Lymphotoxin alpha3 induces chemokines and adhesion molecules: insight into the role of LT alpha in inflammation and lymphoid organ development. J. Immunol. 1998;161:6853–60.
[6] Cuff CA, Sacca R, Ruddle NH. Differential induction of adhesion molecule and chemokine expression by LTalpha3 and LTalphabeta in inflammation elucidates potential mechanisms of mesenteric and peripheral lymph node development. J. Immunol. 1999;162:5965–72.
[7] Kratz A, Campos-Neto A, Hanson MS, Ruddle NH. Chronic inflammation caused by lymphotoxin is lymphoid neogenesis. J. Exp. Med. 1996;183:1461–72.
[8] Koni PA, Sacca R, Lawton P, Browning JL, Ruddle NH, Flavell RA. Distinct roles in lymphoid organogenesis for lymphotoxins alpha and beta revealed in lymphotoxin beta-deficient mice. Immunity 1997;6:491–500.
[9] Schrama D, thor Straten P, Fischer WH, McLellan AD, Brocker EB, Reisfeld RA, et al. Targeting of lymphotoxin-alpha to the tumor elicits an efficient immune response associated with induction of peripheral lymphoid-like tissue. Immunity 2001;14:111–21.
[10] Schrama D, Voigt H, Eggert AO, Xiang R, Zhou H, Schumacher TN, et al. Immunological tumor destruction in a murine melanoma model by targeted LTalpha independent of secondary lymphoid tissue. Cancer Immunol. Immunother. 2008;57:85–95.
[11] Neumann B, Luz A, Pfeffer K, Holzmann B. Defective Peyer's patch organogenesis in mice lacking the 55-kD receptor for tumor necrosis factor. J. Exp. Med. 1996;184:259–64.
[12] Ware CF. Targeting the LIGHT-HVEM pathway. Adv. Exp. Med. Biol. 2009;647: 146–55.
[13] Reisfeld RA, Gillies SD, Mendelsohn J, Varki NM, Becker JC. Involvement of B lymphocytes in the growth inhibition of human pulmonary melanoma metastases in athymic nu/nu mice by an antibody-lymphotoxin fusion protein. Cancer Res. 1996;56:1707–12.
[14] Wang FH, Li YH, Li S, Jiang WQ, Guan ZZ. Phase I clinical trial of intravenous recombinant human lymphotoxin-alpha derivative. Ai. Zheng. 2006;25:501–4.
[15] Yoshioka Y, Tsutsumi Y, Nakagawa S, Mayumi T. Recent progress on tumor missile therapy and tumor vascular targeting therapy as a new approach. Curr. Vasc. Pharmacol. 2004;2:259–70.
[16] Mukai Y, Yoshioka Y, Tsutsumi Y. Phage display and PEGylation of therapeutic proteins. Comb. Chem. High. Throughput Screen 2005;8:145–52.
[17] Fang J, Nakamura H, Maeda H. The EPR effect: Unique features of tumor blood vessels for drug delivery, factors involved, and limitations and augmentation of the effect. Adv. Drug. Deliv. Rev. 2011;63:136–51.

[18] Wang YS, Youngster S, Grace M, Bausch J, Bordens R, Wyss DF. Structural and biological characterization of pegylated recombinant interferon alpha-2b and its therapeutic implications. Adv. Drug. Deliv. Rev. 2002;54: 547–70.
[19] Yamamoto Y, Tsutsumi Y, Yoshioka Y, Nishibata T, Kobayashi K, Okamoto T, et al. Site-specific PEGylation of a lysine-deficient TNF-alpha with full bioactivity. Nat. Biotechnol. 2003;21:546–52.
[20] Yoshioka Y, Tsutsumi Y, Ikemizu S, Yamamoto Y, Shibata H, Nishibata T, et al. Optimal site-specific PEGylation of mutant TNF-alpha improves its antitumor potency. Biochem. Biophys. Res. Commun. 2004;315:808–14.
[21] Shibata H, Yoshioka Y, Ikemizu S, Kobayashi K, Yamamoto Y, Mukai Y, et al. Functionalization of tumor necrosis factor-alpha using phage display technique and PEGylation improves its antitumor therapeutic window. Clin. Cancer. Res. 2004;10:8293–300.
[22] Yoshioka Y, Watanabe H, Morishige T, Yao X, Ikemizu S, Nagao C, et al. Creation of lysine-deficient mutant lymphotoxin-alpha with receptor selectivity by using a phage display system. Biomaterials 2010;31:1935–43.
[23] Kaneda Y, Tsutsumi Y, Yoshioka Y, Kamada H, Yamamoto Y, Kodaira H, et al. The use of PVP as a polymeric carrier to improve the plasma half-life of drugs. Biomaterials 2004;25:3259–66.

Biochemical and Biophysical Research Communications 415 (2011) 558–562

Contents lists available at SciVerse ScienceDirect

Biochemical and Biophysical Research Communications

journal homepage: www.elsevier.com/locate/ybbrc

Structure–activity relationship of T-cell receptors based on alanine scanning

Shogo Narimatsu [a,1], Yasuo Yoshioka [b,c,*,1], Tomohiro Morishige [a], Xinglei Yao [a,d], Shin-ichi Tsunoda [c,e], Yasuo Tsutsumi [b,c,f], Michael I Nishimura [g], Yohei Mukai [a], Naoki Okada [a], Shinsaku Nakagawa [a,b,*]

[a] Laboratory of Biotechnology and Therapeutics, Graduate School of Pharmaceutical Sciences, Osaka University, 1-6, Yamadaoka, Suita, Osaka 565-0871, Japan
[b] The Center for Advanced Medical Engineering and Informatics, Osaka University, 1-6, Yamadaoka, Suita, Osaka 565-0871, Japan
[c] Laboratory of Biopharmaceutical Research, National Institute of Biomedical Innovation, 7-6-8 Saito-Asagi, Ibaraki, Osaka 567-0085, Japan
[d] Institute of Pharmaceutics, Zhejiang University, 388 Yuhangtang Road, Hangzhou 310058, China
[e] Laboratory of Biomedical Innovation, Graduate school of Pharmaceutical Sciences, Osaka University, 7-6-8 Saito-asagi, Ibaraki, Osaka 567-0085, Japan
[f] Laboratory of Toxicology and Safety Science, Graduate School of Pharmaceutical Sciences, Osaka University, 1-6, Yamadaoka, Suita, Osaka 565-0871, Japan
[g] Division of General Surgery, Department of Surgery, Medical University of South Carolina, Charleston, SC, USA

ARTICLE INFO

Article history:
Received 17 October 2011
Available online 31 October 2011

Keywords:
Alanine-scanning
Melanoma
Protein engineering
T-cell receptor

ABSTRACT

T-cell receptors (TCR) recognize complexes between human leukocyte antigens (HLA) and peptides derived from intracellular proteins. Their therapeutic use for antigen targeting, however, has been hindered by the very low binding affinity of TCRs, typically in the 1- to 100-μM range. Therefore, to construct mutant TCRs with high binding affinity, we need to understand the relationship between the structure and activity of these molecules. Here, we attempted to identify the amino acids of the TCR that are important for binding to the peptide/HLA complex. We used a TCR that recognizes complexes between HLA-A*0201 and the peptide from tyrosinase, antigen overexpressed in melanoma. We changed 16 amino acids in the third complementarity-determining region within the TCR to alanine and examined the effect on binding affinity. Five alanine substitutions decreased the binding affinity to below 10% compared with that of wild-type TCR. In contrast, one alanine substitution caused a faster on-rate and slower off-rate, and increased the binding affinity to three times that of the wild-type TCR. Our results provide fundamental information for constructing mutant TCRs with high binding affinity.

1. Introduction

The T-cell receptor (TCR) is a membrane-bound disulfide-linked heterodimer consisting of an α and a β chain [1–3]. Each chain comprises a constant region and a variable region with four framework regions and three complementarity-determining regions (CDR1 to CDR3) [1–3]. TCRs are expressed on T lymphocytes and recognize small peptide antigens on the surfaces of host cells *via* the major histocompatibility complex [MHC; also called the human leukocyte antigen (HLA) system in humans] [1–3]. These peptides consist of about 10 amino acids derived from intracellularly expressed or exogenous proteins. Accordingly, the use of TCRs for antigen-targeting therapy has been explored. In fact, adoptive immunotherapies that make use of T-cells expressing TCRs against specific intracellular cancer antigens currently represent an area of intense interest in the field of cancer treatment [4–6]. In addition, TCRs conjugated to cytokine may provide novel cytokine therapies, because they also target intracellularly expressed proteins [7–9].

However, TCRs generally exhibit much lower affinities for their peptide-MHC complexes ($K_D = 10^{-4}$–10^{-7} M) than antibodies do for their antigens ($K_D = 10^{-7}$–10^{-12} M) [10,11]. Therefore, to develop TCR-based therapeutic interventions, mutant TCRs with high affinities are needed. One approach to the augmentation of TCR affinity is to selectively alter the amino acids of the CDR1, 2, and 3 loops in the TCRs [12,13]. The amino acids of CDR1 and 2 interface with peptide-MHC complexes, predominantly through the MHC rather than the peptide. In contrast, CDR3 amino acids interact with the peptide as it lies in the MHC groove, leading to the belief that CDR3 is an important region for peptide-MHC complex binding [14,15]. However, which CDR3 amino acids are important for this binding is not yet known.

Here, we used alanine scanning of CDR3 amino acids to determine which amino acids are required for peptide-HLA complex binding. Our results provide fundamental information for constructing mutant TCRs with high binding affinity.

* Corresponding authors at: The Center for Advanced Medical Engineering and Informatics, Osaka University, 1-6, Yamadaoka, Suita, Osaka 565-0871, Japan. Fax: +81 6 6879 8233. (Y. Yoshioka), Laboratory of Biotechnology and Therapeutics, Graduate School of Pharmaceutical Sciences, Osaka University, 1-6, Yamadaoka, Suita, Osaka 565-0871, Japan. Fax: +81 6 6879 8179 (S. Nakagawa).

E-mail addresses: yasuo@phs.osaka-u.ac.jp (Y. Yoshioka), nakagawa@phs.osaka-u.ac.jp (S. Nakagawa).

[1] Each author contributed equally to the work.

0006-291X/$ - see front matter © 2011 Elsevier Inc. All rights reserved.
doi:10.1016/j.bbrc.2011.10.092

2. Materials and methods

2.1. Cloning of TCR chains

We used TCR_{tyr} specific for the complex between HLA-A*0201 and the $tyrosinase_{368-376}$ peptide (YMDGTMSQV) [16–18]. We cloned the extracellular domains of the α and β chain sequences of TCR_{tyr} into pET15b plasmids (Novagen, Darmstadt, Germany) separately. Two-step PCR amplification of the α chain was performed by using three primers: primer 1,5′-gatataccatggcccttgctaagaccac ccagcccatctctatggactcatatgaaggacaagaag-3′; primer 2,5′-ctgatgtgta tatcacagacaaatgcgtgctagacatgaggtctatggac-3′; and primer 3,5′-cc ggatcctggagttattaggaactttctgggctggggaagaagg-3′. By using these three primers, we changed threonine 162 of the TCR_{Tyr} α chain to a cysteine codon and the native inter-chain cysteine codon to a TAA stop codon. In addition, three-step PCR amplification of the β chain was performed by using four primers: primer 4,5′-gatataccatggcc gatgctggaatcacccagagccc-3′; primer 5,5′-acccaaaaggccacactggtgtg cctggccaccggtttcttccctgaccacgtggagctgagctggtgggtgaatgggaaggaggt gcacagtggggtctgcacggacccgcagcccctc-3′; primer 6,5′-ccggatcctcga gttattagtctgctctaccccaggcctcggc-3′; and primer 7,5′-gaccctcaggc ggctgctcagagcgtatctggagtcattgagggcgggctgctccttgaggggctgcgggtccg tgcag-3′. By using these 4 primers, we changed serine 177 of the TCR_{Tyr} β chain to a cysteine codon; we also changed the native inter-chain cysteine codon to a TAA stop codon and cysteine 195 of the TCR_{Tyr} β chain, which is not used for disulfide binding, to an alanine codon.

2.2. Expression and refolding of TCR_{tyr} protein

pET15b plasmids separately encoding the α and β chains were prepared and used to transform *Escherichia coli* BL21(DE3) cells (Stratagene, Cedar Creek, TX) for the expression of recombinant proteins. Expression was induced by adding 1 mM Isopropyl β-D-1-thiogalactpyranoside and incubating at 37 °C for 6 h in Terrific Broth (Invitrogen, Carlsbad, CA) containing 0.4% glucose, 1.68 mM MgSO4, and 100 mg/mL ampicillin; all products accumulated as inclusion bodies. Inclusion bodies prepared from cell lysates were washed in 25% Triton-X 100 and solubilized in 6 M guanidine–HCl, 10 mM dithiothreitol, and 10 mM ethylenediaminetetra-acetate, buffered with 50 mM Tris (pH 8.1). TCR_{tyr} was refolded by rapid dilution of a mixture of the dissolved α and β chain inclusion bodies into 5 M urea, 0.4 M L-arginine, 100 mM Tris (pH 8.1), 3.7 mM cystamine, and 6.6 mM β-mercapoethylamine to a final concentration of 60 mg/L for 36 h at 4 °C.

2.3. Purification of TCR_{tyr} protein

After being dialyzed against demineralized water and 10 mM Tris (pH 8.1) at 4 °C, the refolded proteins were filtered and purified by use of ion-exchange chromatography (Q Sepharose Fast Flow; GE Healthcare, Buckinghamshire, UK). The column was washed with 10 mM Tris (pH 8.1) before elution with a 0- to 500-mM NaCl gradient in the same buffer. The elutes were further purified over a HiLoad Superdex 200PG column (GE Healthcare) equilibrated with PBS (pH 7.4). Fractions comprising the main peak were pooled and analyzed further. Sodium dodecyl sulfate polyacrylamide gel electrophoresis (SDS–PAGE) analysis of the final purified TCR_{tyr} was conducted under reducing and non-reducing conditions; proteins were stained with Coomassie brilliant blue (CBB).

2.4. Determination of binding affinity by using surface plasmon resonance (SPR) analysis

SA Sensor chips (BIAcore, St Albans, UK) were coated with streptavidin covalently immobilized on a carboxymethylated dextran matrix, and $tyrosinase_{368-376}$/HLA-A*0201 complexes conjugated to biotin (MBL, Nagoya, Japan) were passed over individual flow cells until the response measured about 1000 response units (RU). TCR_{tyr} protein diluted in HBS-EP running buffer (GE Healthcare) was passed over the $tyrosinase_{368-376}$/HLA-A*0201 complexes for 2 min at a flow rate of 20 μL/min. During the dissociation phase, HBS-EP was run over the sensor chip for 10 min at a flow rate of 20 μL/min. The data obtained were evaluated by using BIAevaluation 4.1 software (GE Healthcare) to apply a 1:1 Langmuir binding model. The sensorgrams were fitted globally over the range of injected concentrations and simultaneously over the association and dissociation phases. To evaluate specificity, we also conducted experiments with MART-1 $peptide_{26-35}$ (ELAGIGILTV)/HLA-A*0201 complexes conjugated to biotin (MBL).

2.5. Generation of alanine scanning TCR_{tyr} mutants

To create alanine scanning TCR_{tyr} mutants, we used the α and β chains in the pET15b plasmids as templates with a KOD-plus mutagenesis kit (Toyobo, Osaka, Japan), according to the manufacturer's instructions. The following four amino acid residues of the α chain CDR3 (Lα90, Vα91, Aα92, and Lα93) and 12 amino acid residues of the β chain CDR3 (Aβ93, Iβ94, Sβ95, Pβ96, Tβ97, Eβ98, Eβ99, Gβ100, Gβ101, Lβ102, Iβ103, and Fβ104) were mutated to alanine. The third amino acid of the α chain CDR3 and the first amino acid of the β chain CDR3 were alanine residues initially, so two alanine residues were changed to glycine residues. Together with wild-type TCR_{tyr} ($wtTCR_{tyr}$), the alanine scanning TCR_{tyr} mutants were produced, purified, and confirmed by SDS–PAGE. Their binding kinetics were analyzed by using SPR analysis.

2.6. Statistical analysis

All data are represented as the means ± SD and differences were compared by using Student's t-test.

3. Results and discussion

3.1. Construction of recombinant TCR_{tyr} protein

Several approaches have been used to generate recombinant TCR proteins; however, there is no universally applicable method for the production of a broad range of TCR proteins [19,20]. Boulter et al. developed a generic recombinant TCR protein production method in which disulfide bond-linked TCRs are generated by introducing a cysteine residue within each of the TCR constant regions [21]. Thus, the TCR proteins can refold from inclusion bodies by using *E. coli* to yield large amounts of soluble, stable, and functional TCRs. First, we attempted to generate recombinant TCR_{tyr} proteins by using an *E. coli* system. TCR_{tyr} genes were cloned into the α and β chain constructs that contained engineered cysteines at positions Tα162 and Sβ177, respectively, by a method similar to that of Boulter et al. [21]. In addition, a free cysteine in the constant domain of the β chain was mutated to alanine to facilitate *in vitro* refolding. The α and β chains were expressed by using *E. coli* strain BL21(DE3) cells separately containing the pET15b plasmids that encoded the α and β chains. After the *E. coli* were lysed, the soluble and insoluble fractions were analyzed by using SDS–PAGE, which confirmed that the α and β chains were present only in the insoluble fraction (data not shown). After solubilization and refolding of the inclusion bodies, we purified the TCR_{tyr} by ion exchange and gel filtration chromatography (Fig. 1A). The protein was eluted as a single major peak at an elution time of ~80 min. Examination of the molecular weight markers indicated that the molecular weight of the protein was about 50 kDa. After fractions

corresponding to the main peak were collected and pooled, the purified protein was analyzed by using CBB staining after SDS-PAGE under reducing and non-reducing conditions (Fig. 1B). The α and β chains ran separately under reducing conditions. Under non-reducing conditions, the introduced disulfide bond held the chains together such that they ran as a single band. These results show that the recombinant TCR_{tyr} formed a heterodimer consisting of α and β chains.

3.2. Binding affinity of TCR_{tyr} to tyrosinase$_{368-376}$/HLA-A*0201 complexes

To measure the binding affinity of TCR_{tyr} to tyrosinase$_{368-376}$/HLA-A*0201 complexes, we performed an SPR analysis with a BIAcore 2000. The TCR_{tyr} bound to the tyrosinase$_{368-376}$/HLA-A*0201 complexes (Fig. 1C), but it failed to bind to MART-1_{26-35}/HLA-A*0201 complexes (Fig. 1D). The equilibrium association constant (KD) of TCR_{tyr} to tyrosinase$_{368-376}$/HLA-A*0201 complexes was 2.7 μM (Table 1). This value is almost equivalent to that of TCRs that specifically recognize other peptide-MHC complexes [11]. These results suggest that the recombinant TCR_{tyr} protein has both binding affinity and specificity for tyrosinase$_{368-376}$/HLA-A*0201 complexes.

3.3. Alanine scanning of the 16 amino acids in CDR3

To define the amino acids of CDR3 that are important for deep binding of the tyrosinase$_{368-376}$/HLA-A*0201 complexes, we performed alanine scanning mutagenesis of the TCR_{tyr}. We attempted to create 16 alanine substitutions, which we then purified by ion exchange and gel filtration chromatography (data not shown). We were able to produce all of the desired mutants except for Vα91A. Therefore, we could not assess the role of this mutation. The purified proteins were analyzed by using CBB staining after SDS-PAGE under reducing and non-reducing conditions. The created point mutants formed the same heterodimeric structure that $wtTCR_{tyr}$ formed (data not shown). We confirmed that all substitution mutants could not bind to MART-1_{26-35}/HLA-A*0201 complexes (data not shown). When we examined the interaction of the mutants with tyrosinase$_{368-376}$/HLA-A*0201 complexes (Fig. 2), we found that eight of the substitution mutants, Aα92G, Lα93A, Iβ94A, Pβ96A, Tβ97A, Eβ98A, Iβ103A, and Fβ104A, showed significantly decreased binding responses to the tyrosinase$_{368-376}$/HLA-A*0201 complexes compared with those of $wtTCR_{tyr}$. In particular, Aα92G and Fβ104A did not bind at all. We also found that the KDs of Tβ97A, Eβ98A and Iβ103A decreased to less than 10% relative to $wtTCR_{tyr}$ (Table 1). On the other hand, Sβ95A, Eβ99A, Gβ100A and Lβ102A showed increased binding responses to the tyrosinase$_{368-376}$/HLA-A*0201 complexes compared with those of $wtTCR_{tyr}$. Furthermore, only Gβ100A raised k_{on} and reduced k_{off} compared with those of $wtTCR_{tyr}$, resulting in the highest relative binding affinity (315%). We concluded that Aα92, Tβ97, Eβ98, Gβ100, Iβ103 and Fβ104 were key residues for the interaction of TCR_{tyr} with tyrosinase$_{368-376}$/HLA-A*0201 complexes. In contrast, the relative bindings of the other nine substitutions (Lα90A, Lα93A, Aβ93G, Iβ94A, Sβ95A, Pβ96A, Eβ99A, Gβ101A, and Lβ102A) ranged from 12.8% to 171.7% compared with that in $wtTCR_{tyr}$ (Fig. 2 and Table 1). We concluded that these residues were not important for binding to the tyrosinase$_{368-376}$/HLA-A*0201 complexes.

The detailed crystal structure of the TCR-HLA complex would be useful for understanding binding modes and kinetic behaviors. However, high-resolution crystal structure of the TCR_{tyr}-HLA complex has not yet been solved and the number of different crystal structures of TCR-HLA complexes is very small [22]. In addition, it is difficult to speculate as to the precise interaction mode of a TCR with a given HLA from the crystal structure of other TCR-HLA complexes, because the interaction mode of the TCR, especially CDR3, differs with each HLA [22]. Therefore we could not discuss why only Gβ100A raised k_{on} and reduced k_{off} compared with the k_{on} and k_{off} values of $wtTCR_{tyr}$, resulting in the highest relative binding affinity. Structural information on a large number of TCR-HLA complexes, including that from this study, will help us

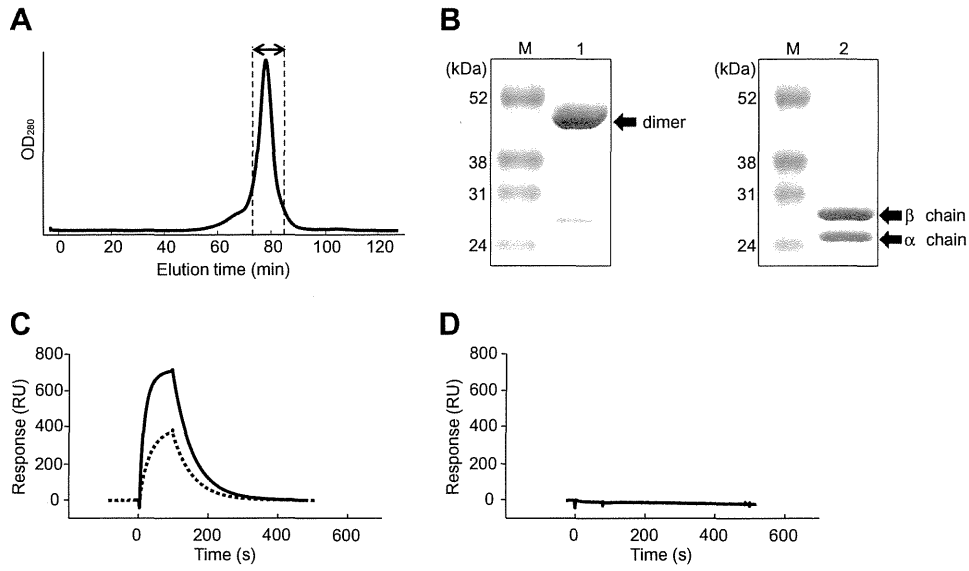

Fig. 1. Construction of $wtTCR_{tyr}$ protein expressed in *E. coli*. (A) Purification of $wtTCR_{tyr}$ by size-exclusion chromatography. Refolded $wtTCR_{tyr}$ was purified by gel filtration chromatography on a Superdex 200PG 16/60 column at a flow rate of 1 mL/min in PBS. (B) SDS-PAGE of pooled fractions. TCR_{tyr} was analyzed by using CBB staining after SDS-PAGE under non-reducing and reducing conditions. Samples were applied to a 4% to 20% SDS-polyacrylamide gel and strained with CBB. Lane M, molecular weight standards; lane 1, $wtTCR_{tyr}$ under non-reducing conditions; lane 2, $wtTCR_{tyr}$ under reducing conditions. Comparison of BIAcore sensorgrams obtained by the binding response to (C) tyrosinase$_{368-376}$/HLA-A*0201 complexes and (D) MART-1_{26-35}/HLA-A*0201 complexes. Duplicate injections of 6.8 μM (—) or 3.4 μM (--) $wtTCR_{tyr}$ were passed over the immobilized peptide/HLA-A*0201 complexes at a flow rate of 20 mL/min. The amount of TCR_{tyr} bound to the peptide/HLA-A*0201 complexes was recorded in response units (RU). The sensorgrams shown were normalized by subtracting the control surface sensorgram.

Table 1
Evaluation of the kinetic parameters of alanine substitution TCR_{tyr} for binding to $tyrosinase_{368-376}$/HLA-A*0201 complexes by using surface plasmon resonance (SPR) analysis. Each kinetic parameter was calculated from the respective sensorgram by using BIA evaluation 4.1 software.

Clone	k_{on} [a] ($\times 10^3$ 1/Ms)	k_{off} [b] ($\times 10^{-3}$ 1/s)	K_D [c] (μM)	Relative binding affinity [d] (%)
$wtTCR_{tyr}$	5.3 ± 0.4	14.2 ± 0.6	2.7 ± 0.1	100
Lα90A	7.3 ± 0.6	22.1 ± 0.8	3.0 ± 0.3	88.7
Aα92G	N.D.	N.D.	N.D.	N.D.
Lα93A	n.d.	n.d.	21.0 ± 1.1**	12.8
Aβ93G	11.1 ± 2.7#	38.6 ± 0.2++	3.6 ± 0.8	75.0
Iβ94A	n.d.	n.d.	17.6 ± 2.0**	15.3
Sβ95A	11.0 ± 2.9#	16.6 ± 0.3++	1.6 ± 0.3**	171.7
Pβ96A	6.8 ± 3.2	76.0 ± 0.3++	12.8 ± 5.3*	21.2
Tβ97A	0.1 ± 0.0##	29.2 ± 3.7++	658.1 ± 63.6**	0.4
Eβ98A	n.d.	n.d.	73.2 ± 15.6**	3.7
Eβ99A	9.9 ± 0.2##	17.7 ± 0.2++	1.8 ± 0.0**	150.4
Gβ100A	9.6 ± 1.9#	8.1 ± 0.1++	0.9 ± 0.1**	314.5
Gβ101A	5.9 ± 1.2	17.3 ± 1.2+	3.0 ± 0.4	90.1
Lβ102A	9.1 ± 1.6#	14.9 ± 0.3	1.7 ± 0.2**	161.5
Iβ103A	n.d.	n.d.	102.1 ± 24.4**	2.6
Fβ104A	N.D.	N.D.	N.D.	N.D.

All data are represented as the means ± SD.
[a] k_{on} is the association kinetic constant.
[b] k_{off} is the dissociation kinetic constant.
[c] K_D is the equilibrium association constant.
[d] Relative binding affinity values are calculated as $100 \times K_D$ ($wtTCR_{tyr}$)/K_D (mutant). N.D., not detectable; n.d., no data.
# $P < 0.05$.
$P < 0.01$ versus value for k_{on} of $wtTCR_{tyr}$.
+ $P < 0.05$.
++ $P < 0.01$ versus value for k_{off} of $wtTCR_{tyr}$.
* $P < 0.05$.
** $P < 0.01$ versus value for K_D of $wtTCR_{tyr}$.

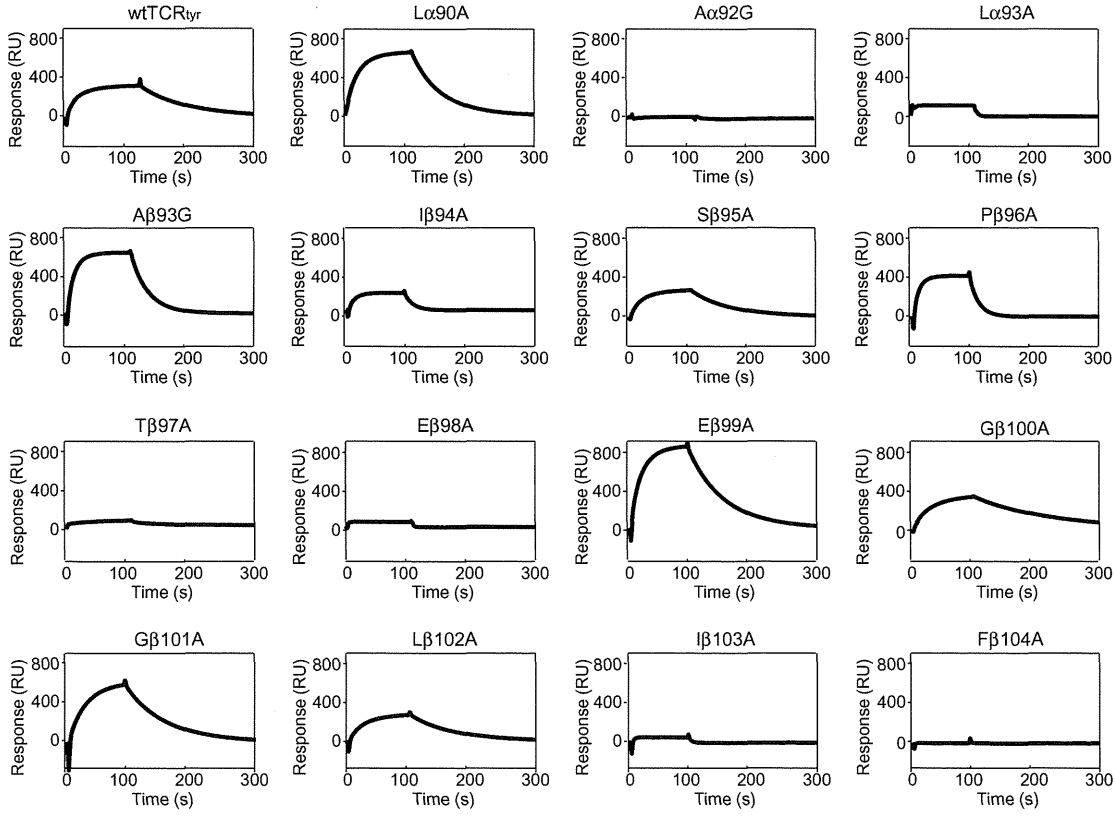

Fig. 2. BIAcore sensorgrams of alanine substitution TCR_{tyr} obtained by the binding response to $tyrosinase_{368-376}$/HLA-A*0201 complexes. Duplicate injections of 3.9 μM TCR_{tyr} were passed over the immobilized peptide/HLA-A*0201 complexes at a flow rate of 20 μL/min. The sensorgrams shown were normalized by subtracting the control surface sensorgram. The amount of protein bound to the surface was recorded in RU.

to understand the precise interaction mode of the TCR with HLA in the future.

Yi Li et al. constructed high-affinity TCRs ($K_D = 2.5 \times 10^{-9}$ M) by using phage display [12]. Their TCRs were generated by extensive mutation of the TCR CDR loops and loop-flanking residues. In contrast, Dunn et al. acquired high-affinity TCRs ($K_D = 1.3 \times 10^{-9}$ M) by mutating only CDR2 amino acids [13]. Although CDR2s contact only the HLA surface and not the bound peptide, the CDR2 mutations did not compromise the selectivity for the bound peptide antigen. We selected CDR3 because its amino acids residues are thought to be most involved in the binding to the peptide-HLA complexes. From here, we plan to similarly characterize the amino acids of CDR1 and 2 to provide the same basic information about them as we were able to obtain about the amino acids of CDR3.

Here, we defined several important amino acids for peptide-HLA complex binding by using alanine scanning of CDR3 amino acids. We showed that the binding affinities of five alanine substitutions dropped to below 10% compared with that of $wtTCR_{tyr}$. Furthermore, one alanine substitution reduced the dissociation kinetic constant compared with that of $wtTCR_{tyr}$ and, as a result, improved the binding affinity. We believe that these results provide basic information of value for a variety of potential biomedical applications of TCRs.

Acknowledgments

The authors declare no conflict of interests. This study was supported in part by grants from the Ministry of Health, Labor, and Welfare of Japan; by a Research on Health Sciences Focusing on Drug Innovation grant from the Japan Health Sciences Foundation; and by the Global COE Program "In Silico Medicine" at Osaka University.

References

[1] R.K. Wilson, E. Lai, P. Concannon, R.K. Barth, L.E. Hood, Structure, organization and polymorphism of murine and human T-cell receptor alpha and beta chain gene families, Immunol. Rev. 101 (1988) 149–172.
[2] J.L. Strominger, Developmental biology of T cell receptors, Science 244 (1989) 943–950.
[3] S.J. Turner, P.C. Doherty, J. McCluskey, J. Rossjohn, Structural determinants of T-cell receptor bias in immunity, Nat. Rev. Immunol. 6 (2006) 883–894.
[4] H.W. Kessels, M.C. Wolkers, M.D. van den Boom, M.A. van der Valk, T.N. Schumacher, Immunotherapy through TCR gene transfer, Nat. Immunol. 2 (2001) 957–961.
[5] C. Rossig, C.M. Bollard, J.G. Nuchtern, C.M. Rooney, M.K. Brenner, Epstein-Barr virus-specific human T lymphocytes expressing antitumor chimeric T-cell receptors: potential for improved immunotherapy, Blood 99 (2002) 2009–2016.
[6] V. Karanikas, C. Lurquin, D. Colau, N. van Baren, C. De Smet, B. Lethe, T. Connerotte, V. Corbiere, M.A. Demoitie, D. Lienard, B. Dreno, T. Velu, T. Boon, P.G. Coulie, Monoclonal anti-MAGE-3 CTL responses in melanoma patients displaying tumor regression after vaccination with a recombinant canarypox virus, J. Immunol. 171 (2003) 4898–4904.
[7] K.F. Card, S.A. Price-Schiavi, B. Liu, E. Thomson, E. Nieves, H. Belmont, J. Builes, J.A. Jiao, J. Hernandez, J. Weidanz, L. Sherman, J.L. Francis, A. Amirkhosravi, H.C. Wong, A soluble single-chain T-cell receptor IL-2 fusion protein retains MHC-restricted peptide specificity and IL-2 bioactivity, Cancer Immunol. Immunother. 53 (2004) 345–357.
[8] H.J. Belmont, S. Price-Schiavi, B. Liu, K.F. Card, H.I. Lee, K.P. Han, J. Wen, S. Tang, X. Zhu, J. Merrill, P.A. Chavillaz, J.L. Wong, P.R. Rhode, H.C. Wong, Potent antitumor activity of a tumor-specific soluble TCR/IL-2 fusion protein, Clin. Immunol. 121 (2006) 29–39.
[9] J. Wen, X. Zhu, B. Liu, L. You, L. Kong, H.I. Lee, K.P. Han, J.L. Wong, P.R. Rhode, H.C. Wong, Targeting activity of a TCR/IL-2 fusion protein against established tumors, Cancer Immunol. Immunother. 57 (2008) 1781–1794.
[10] S.S. Khandekar, P.P. Brauer, J.W. Naylor, H.C. Chang, P. Kern, J.R. Newcomb, K.P. Leclair, H.S. Stump, B.M. Bettencourt, E. Kawasaki, J. Banerji, A.T. Profy, B. Jones, Affinity and kinetics of the interactions between an alphabeta T-cell receptor and its superantigen and class II-MHC/peptide ligands, Mol. Immunol. 34 (1997) 493–503.
[11] D.K. Cole, N.J. Pumphrey, J.M. Boulter, M. Sami, J.I. Bell, E. Gostick, D.A. Price, G.F. Gao, A.K. Sewell, B.K. Jakobsen, Human TCR-binding affinity is governed by MHC class restriction, J. Immunol. 178 (2007) 5727–5734.
[12] Y. Li, R. Moysey, P.E. Molloy, A.L. Vuidepot, T. Mahon, E. Baston, S. Dunn, N. Liddy, J. Jacob, B.K. Jakobsen, J.M. Boulter, Directed evolution of human T-cell receptors with picomolar affinities by phage display, Nat. Biotechnol. 23 (2005) 349–354.
[13] S.M. Dunn, P.J. Rizkallah, E. Baston, T. Mahon, B. Cameron, R. Moysey, F. Gao, M. Sami, J. Boulter, Y. Li, B.K. Jakobsen, Directed evolution of human T cell receptor CDR2 residues by phage display dramatically enhances affinity for cognate peptide-MHC without increasing apparent cross-reactivity, Protein Sci. 15 (2006) 710–721.
[14] J.B. Reiser, C. Darnault, C. Gregoire, T. Mosser, G. Mazza, A. Kearney, P.A. van der Merwe, J.C. Fontecilla-Camps, D. Housset, B. Malissen, CDR3 loop flexibility contributes to the degeneracy of TCR recognition, Nat. Immunol. 4 (2003) 241–247.
[15] J. Zhou, R. Ma, R. Luo, Y. Sun, X. He, W. Sun, W. Tang, X. Yao, Primary exploration of CDR3 spectratyping and molecular features of TCR beta chain in the peripheral blood and tissue of patients with colorectal carcinoma, Cancer Epidemiol 34, 733–740.
[16] M.I. Nishimura, D. Avichezer, M.C. Custer, C.S. Lee, C. Chen, M.R. Parkhurst, R.A. Diamond, P.F. Robbins, D.J. Schwartzentruber, S.A. Rosenberg, MHC class I-restricted recognition of a melanoma antigen by a human CD4+ tumor infiltrating lymphocyte, Cancer Res. 59 (1999) 6230–6238.
[17] M.I. Nishimura, J.J. Roszkowski, T.V. Moore, N. Brasic, M.D. McKee, T.M. Clay, Antigen recognition and T-cell biology, Cancer Treat. Res. 123 (2005) 37–59.
[18] R.C. Koya, S. Mok, B. Comin-Anduix, T. Chodon, C.G. Radu, M.I. Nishimura, O.N. Witte, A. Ribas, Kinetic phases of distribution and tumor targeting by T cell receptor engineered lymphocytes inducing robust antitumor responses, Proc. Natl. Acad. Sci. USA 107 14286–14291.
[19] B.E. Willcox, G.F. Gao, J.R. Wyer, J.E. Ladbury, J.I. Bell, B.K. Jakobsen, P.A. van der Merwe, TCR binding to peptide-MHC stabilizes a flexible recognition interface, Immunity 10 (1999) 357–365.
[20] B.E. Willcox, G.F. Gao, J.R. Wyer, C.A. O'Callaghan, J.M. Boulter, E.Y. Jones, P.A. van der Merwe, J.I. Bell, B.K. Jakobsen, Production of soluble alphabeta T-cell receptor heterodimers suitable for biophysical analysis of ligand binding, Protein Sci. 8 (1999) 2418–2423.
[21] J.M. Boulter, M. Glick, P.T. Todorov, E. Baston, M. Sami, P. Rizkallah, B.K. Jakobsen, Stable, soluble T-cell receptor molecules for crystallization and therapeutics, Protein Eng. 16 (2003) 707–711.
[22] L. Varani, A.J. Bankovich, C.W. Liu, L.A. Colf, L.L. Jones, D.M. Kranz, J.D. Puglisi, K.C. Garcia, Solution mapping of T cell receptor docking footprints on peptide-MHC, Proc. Natl. Acad. Sci. USA 104 (2007) 13080–13085.

Laboratory of Biopharmaceutical Research[1], National Institute of Biomedical Innovation; Laboratory of Toxicology and Safety Science[2], Graduate School of Pharmaceutical Sciences; The Center for Advanced Medical Engineering and Informatics[3]; Laboratory of Biomedical Innovation[4], Graduate School of Pharmaceutical Sciences, Osaka University, Osaka, Japan

Rho GDP-dissociation inhibitor alpha is associated with cancer metastasis in colon and prostate cancer

T. YAMASHITA[1,2,*], T. OKAMURA[1,*], K. NAGANO[1,*], S. IMAI[1], Y. ABE[1], H. NABESHI[1,2], T. YOSHIKAWA[1,2], Y. YOSHIOKA[1,2,3], H. KAMADA[1,3], Y. TSUTSUMI[1,2,3], S. TSUNODA[1,3,4]

Received July 7, 2011, accepted August 5, 2011

Shin-ichi Tsunoda, Ph.D, Laboratory of Biopharmaceutical Research, National Institute of Biomedical Innovation, 7-6-8 Saito-Asagi, Ibaraki, Osaka 567-0085, Japan.
tsunoda@nibio.go.jp
**These authors contributed equally to the work.*

Pharmazie 67: 253–255 (2012) *doi: 10.1691/ph.2012.1630*

Since metastasis is one of the most important prognostic factors in colorectal cancer, development of new methods to diagnose and prevent metastasis is highly desirable. However, the molecular mechanisms leading to the metastatic phenotype have not been well elucidated. In this study, a proteomics-based search was carried out for metastasis-related proteins in colorectal cancer by analyzing the differential expression of proteins in primary versus metastasis focus-derived colorectal tumor cells. Protein expression profiles were determined using a tissue microarray (TMA), and the results identified Rho GDP-dissociation inhibitor alpha (Rho GDI) as a metastasis-related protein in colon and prostate cancer patients. Consequently, Rho GDI may be useful as a diagnostic biomarker and/or a therapeutic to prevent colon and prostate cancer metastasis.

1. Introduction

Colorectal cancer is known as a major metastatic cancer, and 40–50% of patients already have a metastatic focus at presentation. Moreover, the 5-year survival of these patients is under 10% (Davies et al. 2005). Thus, metastasis is one of the most important prognostic factors in colorectal cancer. In order to improve rates of cancer remission, it will be necessary to clarify the detailed molecular mechanisms of cancer metastasis and to utilize this information to establish new diagnostic and therapeutic techniques. Many researchers have searched for metastasis-related molecules (Liu et al. 2010; Shuehara et al. 2011) using proteomics techniques (Hanash 2003). Comprehensive mapping of the molecular changes during metastasis would greatly improve our understanding of the recurrence and management of cancer. However, the knowledge gained so far in these studies has not been sufficient to improve cancer remission rates.

Here we show the potential of Rho GDI as a metastasis-related protein in colon and prostate cancer patients. In order to identify metastasis-related proteins, the protein expression patterns of human colorectal cancer cells with different metastatic characters were compared. Because these cells were derived from the same patient (SW480: a surgical specimen of a primary colon adenocarcinoma, SW620: a lymph node metastatic focus), cancer metastasis-related protein candidates could be effectively sought without background variations due to differences between individuals. Furthermore, by analyzing the expression of candidate proteins in many clinical samples using a TMA, we attempted to validate the association of these candidates with metastasis. TMA is a slide glass containing many clinical tissues, and it enables one to carry out a high-throughput analysis by evaluating the relationship between expression profiles of each candidate molecule and clinical information such as metastasis. (Imai et al. 2011; Yoshida et al. 2011).

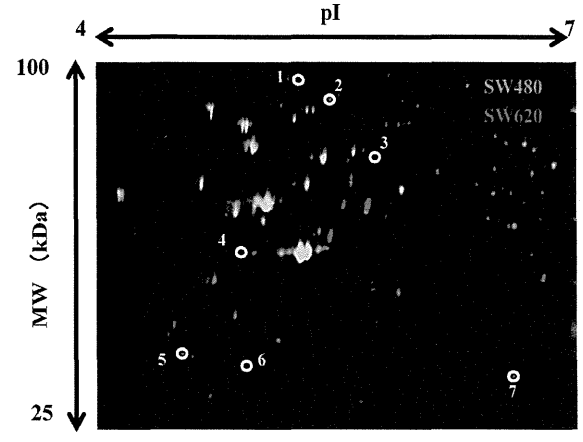

Fig. 1: 2D-DIGE image of fluorescently-labeled proteins from different metastatic human colorectal cancer cells. SW480 is human colorectal cancer cell line derived from a primary tumor and SW620 is derived from a metastatic focus from the same patient. Proteins from the colon cancer cells (SW480, SW620) were labeled with Cy3 and Cy5 respectively, and analyzed by 2D electrophoresis. The differentially-expressed spots (white circles) were then identified by LC-UHR TOF/MS

Table 1: High expression proteins in SW620 compared to SW480

	Accession	Protein name	MW (kDa)	pI	Ratio (SW620 / SW480)
1	P12109	collagen alpha-1(VI) chain	108.6	5.3	1.53
2	Q15459	splicing factor 3A subunit 1	88.9	5.2	1.61
3	P13797	T-plastin	70.9	5.5	1.59
4	P60709	actin cytoplasmic 1	42.1	5.3	1.50
5	P63104	14-3-3 zeta/delta	27.9	4.7	1.63
6	P52565	Rho GDP-dissociation inhibitor 1 (Rho GDI)	23.3	5.0	1.90
7	P30041	Peroxiredoxin-6 (PRDX6)	25.1	6.0	1.86

2. Investigations, results and discussion

In order to search for metastasis-related proteins, we analyzed differentially-expressed proteins between SW480 and SW620 by two-dimensional differential in-gel electrophoresis (2D-DIGE) (Fig. 1). As a result, 7 spots with at least a 1.5-fold-altered expression level were found by quantitative analysis, and these spots were identified by mass spectrometry (Table 1). Three molecules having a high SW620/SW480 expression ratio indicating a strong association with cancer metastasis were identified: Rho GDP-dissociation inhibitor alpha (Rho GDI), peroxiredoxin-6 (PRDX6) and 14-3-3 zeta/delta.

The expression profiles of these proteins were analyzed by immunohistochemistry using the TMA with colon cancer and multiple cancer tissues. Results of this analysis indicated that expression of PRDX6 and 14–3-3 zeta/delta had no relationship to the clinical status of cancer metastasis (data not shown). On the other hand, in positive cases of lymph node metastasis, the expression ratio of Rho GDI was significantly higher than in the negative cases. Furthermore, the same trend was seen when tissues from prostate cancer patients were analyzed (Table 2).

To confirm these results, the expression levels of Rho GDI protein in colon cancer cell lines with different metastatic potential (SW480 < SW620 < SW620-OK1 < SW620-OK2: Characteristics of SW620-OK1 and SW620-OK2 are described in *Experimental*) were investigated by western blot analysis (Fig. 2). The expression of Rho GDI was found to be up-regulated with the development of metastatic characteristics. These results suggested that Rho GDI is correlated with cancer metastasis.

Rho GDI has been identified as key regulator of Rho family GTPases. Activation of growth factor receptors and integrins can promote the exchange of GDP for GTP on Rho proteins (Bishop et al. 2000). Furthermore, GTP-bound Rho proteins interact with a range of effector molecules to modulate their activity or localization, and this leads to changes in cell behavior. It is clear that Rho family GTPases are involved in the control of cell morphology and motility (Etienne-Manneville et al. 2002; Hall et al. 1997; Van Aelst et al. 1997). The importance of Rho protein and Rho GDI in cancer progression, particularly in the area of metastasis, is becoming increasingly evident. Recently, some reports have indicated that the expression of Rho GDI was correlated with colorectal and breast cancer metastasis (Zhao et al. 2008; Kang et al. 2010). Thus, our findings are consistent with these reports and further suggest that the expression of Rho GDI is also correlated with prostate cancer metastasis. Consequently, Rho GDI should be considered as a diagnostic marker or new therapeutic target for cancer metastasis.

3. Experimental

3.1. Cell lines

SW480 is a human colorectal cancer cell line derived from a primary focus and SW620 is derived from a metastatic focus of the same patient. These cells were purchased from American Type Culture Collection and maintained at 37 °C using Leibovitz's L-15 medium (Wako) supplemented with 10% FCS. SW620-OK1 and -OK2 were established by the following procedure: 1×10^6 SW620 cells were injected into the spleens of nu/nu mice. After 8 weeks, SW620-OK1 was established from a liver metastatic focus. Furthermore, SW620-OK2 was established from SW620-OK1 using the same procedures.

3.2. 2D-DIGE analysis

Cell lysates were prepared from SW480 and SW620 and then solubilized with 7 M urea, 2 M thiourea, 4% CHAPS and 10 mM Tris-HCl (pH 8.5). The lysates were labeled at the ratio of 50 µg proteins: 400 pmol Cy3 or Cy5 protein-labeling dye (GE Healthcare Biosciences) in dimethylformamide according to the manufacturer's protocol. Briefly, the labelled samples were mixed with rehydration buffer (7 M urea, 2 M thiourea, 4% CHAPS, 2% DTT, 2% Pharmalyte (GE Healthcare Biosciences)) and applied to a 24-cm immobilized pH gradient gel strip (IPG-strip pH 4–7 NL) for separation in the first dimension. Samples for the spot-picking gel were prepared without labelling by Cy-dyes. For the second dimension separation, the IPG-strips were applied to SDS-PAGE gels (10% polyacrylamide and 2.7% N,N'-diallyltartardiamide gels). After electrophoresis, the gels were scanned with a laser fluoroimager (Typhoon Trio, GE Healthcare Biosciences). The spot-picking gel was scanned after staining with Deep Purple Total Protein Stain (GE Healthcare Biosciences). Quantitative analysis of protein spots was carried out with Decyder-DIA software (GE Healthcare Biosciences). For the antigen spots of interest, spots of 1 mm × 1 mm in size were picked using Ettan Spot Picker (GE Healthcare Biosciences).

3.3. In-gel tryptic digestion

Picked gel pieces were digested with trypsin as described below. The gel pieces were destained with 50% acetonitrile/50 mM NH_4HCO_3 for 20 min twice, dehydrated with 75% acetonitrile for 20 min, and then dried using a centrifugal concentrator. Next, 5 µl of 20 µl/ml trypsin (Promega) solution was added to each gel piece and incubated for 16 h at 37 °C. Three solutions were used to extract the resulting peptide mixtures from the gel pieces. First, 50 µl of 50% (v/v) acetonitrile in 0.1% (v/v) formic acid (FA) was added to the gel pieces, which were then sonicated for 5 min. Next, we collected the solution and added 80% (v/v) acetonitrile in 0.1% FA. Finally, 100% acetonitrile was added for the last extraction. The peptides were dried and then re-suspended in 10 µl of 0.1% FA.

3.4. Mass spectrometry and database search

Extracted peptides were analyzed by liquid chromatography Ultra High Resolution time-of-flight mass spectrometry (LC-UHR TOF/MS; maXis, Bruker Daltonics). The Mascot search engine (http://www.matrixscience.com) was initially used to query the entire theoretical tryptic peptide database as well as SwissProt (http://www.expasy.org/, a public domain database pro-

Table 2: Expression profile of Rho GDI in primary cancers with or without lymph node metastasis

	Number of Rho GDI positive cases (positive ratio)	
	in metastasis negative cases	in metastasis positive cases
Colon cancer*	11/14 (79%)	19/19 (100%)
Prostate cancer*	18/23 (78%)	11/11 (100%)

* $p < 0.05$: Mann Whitney U test

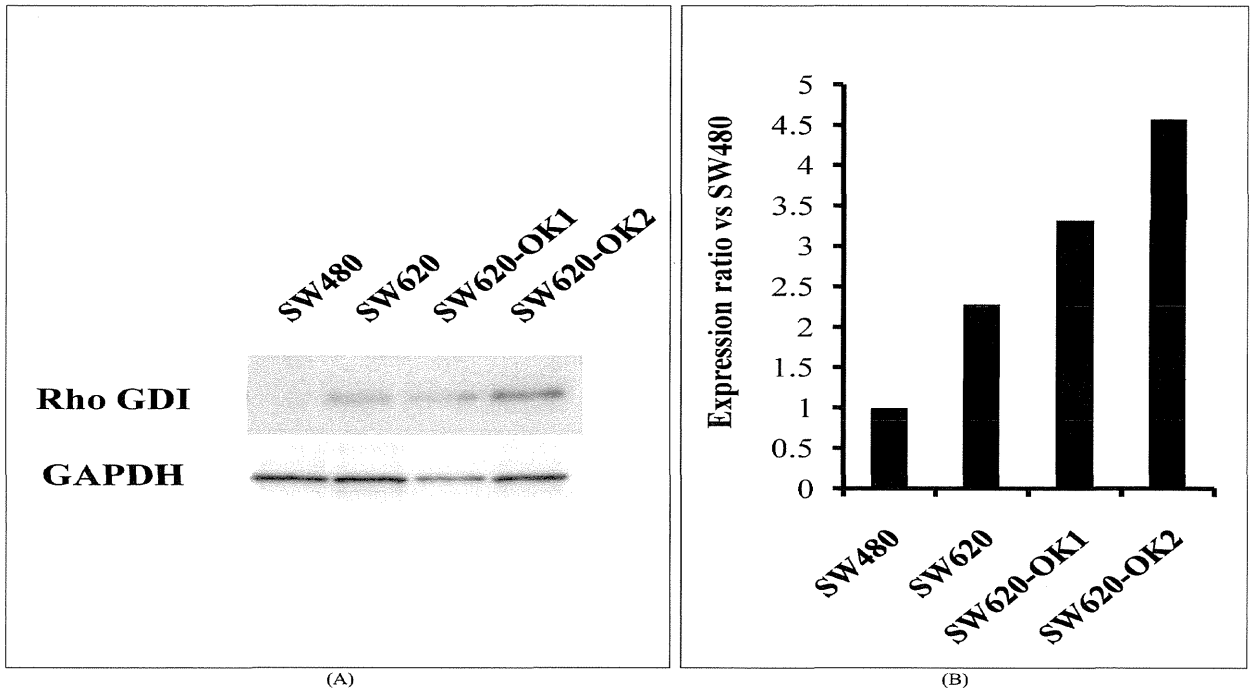

Fig. 2: Rho GDI expression levels in colon cancer cell lines with different metastatic abilities. Rho GDI expression levels in colon cancer cell lines (SW480, SW620, SW620-OK1, SW620-OK2) analyzed by western blotting (A). SW620-OK1, SW620-OK2 have been established as high metastatic sub-lines of SW620 using a mouse metastasis model. Intensity of the western blotting images was quantified by densitometry (B)

vided by the Swiss Institute of Bioinformatics). The search query assumed the following: (i) the peptides were monoisotopic (ii) methionine residues may be oxidized (iii) all cysteines are modified with iodoacetamide.

3.5. TMA Immunochemical staining

TMA slides with human colon cancer samples or multiple cancer samples (Biomax) were de-paraffinated in xylene and rehydrated in a graded series of ethanol washes. Heat-induced epitope retrieval was performed while maintaining the Target Retrieval Solution pH 9 (Dako) at the desired temperature according to manufacturer's instructions. After the treatment, endogenous peroxidase was blocked with 0.3% H_2O_2 in Tris-buffer saline (TBS) for 5 min. After washing twice with TBS, TMA slides were incubated with 10% BSA blocking solution for 30 min. The slides were then incubated with the anti-Rho GDI (Santa Cruz Biotechnology) for 60 min. After washing three times with wash buffer (Dako), each series of sections was incubated for 30 min with Envision + Dual Link (Dako). The reaction products were rinsed twice with wash buffer and then developed in liquid 3, 3'-diaminobenzidine (Dako) for 3 min. After the development, sections were counterstained with Mayer's hematoxylin. All procedures were performed using AutoStainer (Dako).

3.6. TMA Immunohistochemistry scoring

The optimized staining conditions for TMAs corresponding to human colon as well as multiple cancers were determined based on the co-existence of both positive and negative cells in the same tissue sample. Signals were considered positive when reaction products were localized in the expected cellular component. The criteria for scoring of stained tissues were as follows: the distribution score was 0 (0%), 1 (1–50%) or 2 (51–100%), indicating the percentage of positive cells among all tumor cells present in one tissue. The intensity of the signal (intensity score) was scored as 0 (no signal), 1 (weak), 2 (moderate) or 3 (marked). The distribution and intensity scores were then summed into a total score (TS) of TS0 (sum = 0), TS1 (sum = 2), TS2 (sum = 3), and TS3 (sum = 4–5). Throughout this study, TS0 or TS1 was regarded as negative, whereas TS2 or TS3 were regarded as positive.

3.7. Western Blot

Expression of Rho GDI in colon cancer cells was detected by anti-Rho GDI (Santa Cruz Biotechnology) and HRP conjugated anti-mouse IgG antibody (Sigma) using the ECL-plus system. Equal amounts of protein loading were confirmed by parallel β-actin immunoblotting, and signal quantification was performed by densitometric scanning.

Acknowledgements: This study was supported in part by Grants-in-Aid for Scientific Research from the Ministry of Education, Culture, Sports, Science and Technology of Japan, and from the Japan Society for the Promotion of Science (JSPS). This study was also supported in part by Health Labor Sciences Research Grants from the Ministry of Health, Labor and Welfare of Japan.

References

Bishop AL, Hall A (2000) Rho GTPases and their effector proteins. Biochem J 348: 241–255.

Davies RJ, Miller R, Coleman N (2005) Colorectal cancer screening: prospects for molecular stool analysis. Nat Rev Cancer 5: 199–209.

Etienne-Manneville S, Hall A (2002) Rho GTPases in cell biology. Nature 420: 629–635.

Hall A (1997). Rho GTPases and the Actin cytoskeleton. Science 279: 509–514.

Hanash S (2003) Disease proteomics. Nature 422: 226–232.

Imai S, Nagano K, Yoshida Y, Okamura T, Yamashita T, Abe Y, Yoshikawa T, Yoshioka Y, Kamada H, Mukai Y, Nakagawa S, Tsutsumi Y, Tsunoda S (2011). Development of an antibody proteomics system using a phage antibody library for efficient screening of biomarker proteins. Biomaterials 32: 162–169.

Kang S, Kim MJ, An H, Kim BG, Choi YP, Kang KS, Gao MQ, Park H, Na HJ, Kim HK, Yun HR, Kim DS, Cho NH (2010) Proteomic molecular portrait of interface zone in breast cancer. J Proteome Res 9: 5638–5645.

Liu R, Wang K, Yuan K, Wei Y, Huang C (2010) Integrative oncoproteomics strategies for anticancer drug discovery. Expert Rev Proteomics 7: 411–429.

Sahai E (2007). Illuminating the metastatic process. Nat Rev Cancer 7: 737–749.

Suehara Y, Tochigi N, Kubota D, Kikuta K, Nakayama R, Seki K, Yoshida A, Ichikawa H, Hasegawa T, Kaneko K, Chuman H, Beppu Y, Kawai A, Kondo T (2011) Secernin-1 as a novel prognostic biomarker candidate of synovial sarcoma revealed by proteomics. J Proteomics 74: 829–842.

Van Aelst L, D'Souza-Schorey C (1997) Rho GTPases and signaling networks. Genes Dev 11: 2295–2322.

Yoshida Y, Yamashita T, Nagano K, Imai S, Nabeshi H, Yoshikawa T, Yoshioka Y, Abe Y, Kamada H, Tsutsumi Y, Tsunoda S (2011) Limited expression of reticulocalbin-1 in lymphatic endothelial cells in lung tumor but not in normal lung. Biochem Biophys Res Commun 405: 610–614.

Zhao L, Wang H, Li J, Liu Y, Ding Y (2008) Overexpression of Rho GDP-dissociation inhibitor alpha is associated with tumor progression and poor prognosis of colorectal cancer. J Proteome Res 7: 3994–4003.

Yoshioka et al. Chemistry Central Journal 2011, 5:25
http://journal.chemistrycentral.com/content/5/1/25

Chemistry Central Journal

REVIEW Open Access

Development of a novel DDS for site-specific PEGylated proteins

Yasuo Yoshioka[1,2,3], Shin-ichi Tsunoda[2,3,4*] and Yasuo Tsutsumi[1,2,3*]

Abstract

Because of the shifted focus in life science research from genome analyses to genetic and protein function analyses, we now know functions of numerous proteins. These analyses, including those of newly identified proteins, are expected to contribute to the identification of proteins of therapeutic value in various diseases. Consequently, pharmacoproteomic-based drug discovery and development of protein therapies attracted a great deal of attention in recent years. Clinical applications of most of these proteins are, however, limited because of their unexpectedly low therapeutic effects, resulting from the proteolytic degradation *in vivo* followed by rapid removal from the circulatory system. Therefore, frequent administration of excessively high dose of a protein is required to observe its therapeutic effect *in vivo*. This often results in impaired homeostasis *in vivo* and leads to severe adverse effects. To overcome these problems, we have devised a method for chemical modification of proteins with polyethylene glycol (PEGylation) and other water-soluble polymers. In addition, we have established a method for creating functional mutant proteins (muteins) with desired properties, and developed a site-specific polymer-conjugation method to further improve their therapeutic potency. In this review, we are introducing our original protein-drug innovation system mentioned above.

Introduction

The success of the human genome project has clearly shown that the human genome encodes about 35,000 genes and over half of them are poorly understood proteins. A number of these proteins are thought to be related to pathological disorders and other biological phenomena, and thus, are potentially useful as therapeutic agents and as targets for pharmaceutical development. Therefore, focus in life science research has currently shifted to newer fields, such as proteomics and structural genomics, in which the function and structure of proteins are analyzed *en masse*. Such analyses of large number of proteins, including the newly identified proteins, are expected to contribute to the identification of proteins of therapeutic importance in various diseases. In recent years, protein therapies using cytokines or antibodies have attracted a great deal of attention. Indeed, attempts are currently under progress to develop a wide range of therapeutic proteins for treating various diseases including cancer, hepatitis and autoimmune conditions[1-4]. Unfortunately, clinical applications of many of these proteins are limited because of their unexpectedly poor therapeutic effects[5,6]. Often these proteins are degraded by various proteases *in vivo* and rapidly removed from the circulatory system. Consequently, frequent administration of an excessively high dose of a protein is required to obtain its desired therapeutic effect *in vivo*, leading to a disturbance in the homeostasis and unexpected side effects. Additionally, bioactive proteins, such as cytokines, generally show pleiotropic actions through a number of receptors *in vivo*, making it difficult to elicit the desired effect without simultaneously triggering undesirable secondary effects. From this standpoint, creation of novel technologies that overcome the problems peculiar to bioactive proteins is essential for the advancement of pharmacoproteomic-based drug development. These technologies are suitable as Drug Delivery Systems (DDSs), aiming to maximize the therapeutic potency of proteins.

Our laboratory aims to develop novel DDS techniques for overcoming the problems of protein therapy: (i) establishment of a novel polymer-conjugation system to

* Correspondence: tsunoda@nibio.go.jp; ytsutsumi@phs.osaka-u.ac.jp
[1]Department of Toxicology and Safety Science, Graduate School of Pharmaceutical Sciences, Osaka University, 1-6 Yamadaoka, Suita, Osaka 565-0871, Japan
[2]The Center for Advanced Medical Engineering and Informatics, Osaka University, 1-6, Yamadaoka, Suita, Osaka 565-0871, Japan
Full list of author information is available at the end of the article

dramatically improve *in vivo* stability and selectively of bioactive proteins (polymeric DDS) and (ii) development of a powerful system to rapidly create functional mutant proteins (muteins) with enhanced receptor affinity and receptor specificity using a phage display technique (biological DDS). We are currently in the process of combining both approaches to create a protein-drug innovation system to further promote pharmaco-proteomic-based drug development. In this review, we will describe DDS-based technology to create functional mutants for advanced medical applications using the tumor necrosis factor-alpha (TNF) as an example and the usefulness of site-specific polymer-conjugation of proteins.

Bioconjugation as a polymeric DDS

One way to circumvent the problems of protein therapy is to conjugate them with polyethylene glycol (PEG) and other water-soluble polymeric modifiers (Figure 1) [4,7,8]. The covalent conjugation of proteins with PEG (PEGylation) increases their molecular size and steric hindrance, both of which depend on the properties of the PEG attached to the protein. Bioconjugation of proteins decreases their renal excretion rate due to the increased molecular size. In addition, because the polymers cover the protein surface, attack by a protease is generally blocked due to the steric hindrance, thus prolonging the half-life of the protein *in vivo*. The prolonged circulating lifetime in blood induces the enhanced permeability and retention (EPR) effect, which is based on the leaky nature of the tumor blood vessels, resulting in increased delivery of the conjugates to the tumor tissue[9]. Because of all these advantages, it is possible to use the bioactive protein at a decreased dose. However, this approach is limited by the frequent substantial loss of protein specific activity associated with polymer-conjugation. Bioconjugation commonly targets the ε-amino group of lysine residues and/or the N-terminal α-amino group of the protein because they are highly reactive and the bionconjugation reaction is mild

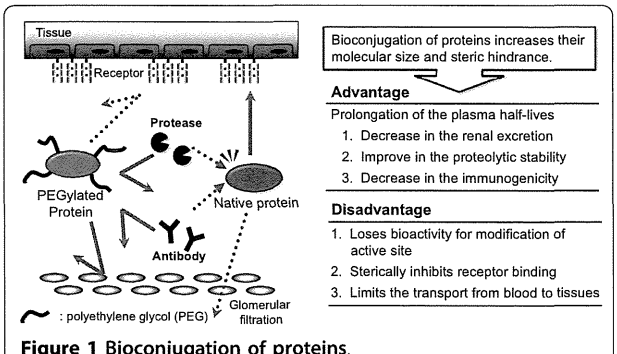

Figure 1 Bioconjugation of proteins.

enough to minimize disruption of the protein structure. Because lysine residues often assume important roles in the formation of multi-dimensional structures and in bonding between ligands and receptors, introduction of polymers at these sites can potentially reduce the biological activity of the protein[10,11]. Indeed, PEGylated interferon, which has raised hopes as a potential cure for hepatitis C, can only be produced as a heterogeneous mixture with 10-30% of the anticipated activity[11].

Tumor necrosis factor-α (TNF-α), an antitumor cytokine, has numerous bioactivities including direct cytotoxicity against tumor cells, activation of immune antitumor response, and selective impairment of tumor-blood vessels[12]. Thus, TNF-α has been considered as a novel antitumor agent[13-15]. However, as a systemic antitumor agent, very high doses of TNF-α were required to obtain sufficient clinical responses, because TNF-α is rapidly cleared from the circulation and also because it becomes widely distributed to various tissues following intravenous administration. As a result, TNF-α with pleiotropic *in vivo* actions exhibited unexpected toxic side-effects, typified by pyrexia and hypertension [16,17]. Systemic application of TNF-α was, therefore, abandoned despite intratumoral administration of TNF-α showing significant antitumor effects in phase I studies[5]. Similar *in vivo* drawbacks are also found in the clinical applications of other bioactive proteins[6]. Keeping these problems in mind, we have devised ways to improve the polymer-conjugation system using the TNF-α as a model protein[18-23]. In PEGylation of TNF-α, the specific activity of PEGylated TNF-α decreased with the degree of PEG-modification (i.e., PEG modification rate). Additionally, when the PEG modification rates are same, the bioactivity of PEGylated TNF-α decreased with an increase in the molecular size of the attached PEG. Thus, when bioactive proteins, such as TNF-α, are able to stably express their activities after binding to polymeric macromolecules, proper attention should be paid to minimize the loss in activity arising from the inhibition of their binding to the receptor molecules due to the steric hindrance posed by the polymeric modifier. By assessing the relationship between the molecular weight of PEG attached to TNF-α, degree of modification of PEG-modified TNF-α, and their *in vivo* antitumor potency, we succeeded in markedly and selectively enhancing the antitumor potency of PEGylated-TNF-α over that of the native TNF-α. Our results suggest that comprehensive analysis of the relationship between the degree of modification by polymer, molecular size, and specific activity could lead to the development of bioconjugated proteins with increased therapeutic value and decreased side effects.

These results suggest that PEGylation is a pragmatic approach for developing successful therapies with drugs,

such as enzymes and antitumor agents. We believe that the technique of bioconjugating drugs to a polymeric carrier will indeed be an important technique for expanding the clinical applications of therapeutic proteins. In this context it is noteworthy that in recent years several research laboratories around the world have created similar polymer-conjugated bioactive proteins. As a result, PEGylated granulocyte-colony stimulating factor (PEG-G-CSF; PEG filgrastim), PEGylated interferon-alpha (PEG-IFN; PEGASYS, PEG-Intron), PEGylated asparaginase (PEG-Asp; ONCASPER), PEGylated adenosine deaminase (PEG-ADA; ADAGEN) and polystyrene-co-maleic acid-conjugated neocarzinostatin (SMANCS) have been developed, all of which showed marked improvement in therapeutic efficacy in comparison to their corresponding native forms[24-28].

A new method for site-specific PEGylation

As described above, PEGylation is limited by the frequent substantial loss of protein specific activity associated with polymer-conjugation. In addition, such bioconjugated proteins could also consist of positional isomers of polymeric modifiers at various sites, each one of which may have distinct activity and other characteristics. Random modification could produce a heterogeneous mixture of conjugated proteins, consisting of different number of modifier molecules bound to various sites of the protein. As a result, functional properties of the bioconjugated proteins (such as activation, *in vivo* behavior, stability) are compromised, and thus, they could exhibit inconsistent therapeutic effects. Therefore, to improve the polymer-conjugation technique in the post-genome era, the pharmaceutical technology would require a method that maintains the present efficiency of polymer modification while simultaneously making the site-specific modification possible. For example, mutant proteins with free cysteine residues were created for modification. However, introduction of cysteine residues led to protein misfolding and aggregation, resulting in unexpected loss of activity. Furthermore, even if it were possible to produce a cysteine mutant that retained activity, the poor efficiency of polymer conjugation to the thiol group made it impossible to obtain the desired product.

To overcome this problem of PEGylation, we have developed a strategy for site-specific PEGylation of TNF-α (Figure 2). Because a deletion mutant of TNF-α lacking eight residues at the N terminus retains full bioactivity, we surmised that the N terminus of TNF-α is not important for function and might therefore be a good target for PEGylation[29]. However, TNF-α contains six internal lysine residues and the amino groups of all six of them are also targets for PEGylation. Site-directed mutagenesis analysis have shown that Lys11

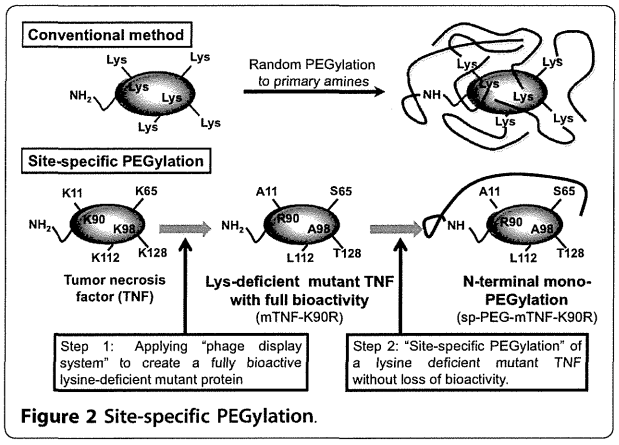

Figure 2 Site-specific PEGylation.

and Lys90 are vital for the bioactivity of TNF-α[30,31]. Nevertheless, if one could construct fully bioactive TNF-α in which all the lysine residues were replaced with other amino acids, site-specific PEGylation of the N-terminus could then be carried out. This PEGylated mutant TNF-α would be expected to have excellent molecular uniformity and retain high bioactivity.

To construct fully bioactive TNF-α in which all the lysine residues were replaced with other amino acids, we employed the "molecular evolution strategy" developed in our laboratory to artificially create functional muteins using our phage display system[32,33]. Phage libraries displaying polypeptides, such as naive antibodies or random peptides, have been extensively used for identifying specific molecules with high affinity for a target ligand [34-36]. The advantages of a phage display system are easy preparation of a library consisting of structural variants of a polypeptide as diverse as over one hundred million and isolation of several targeted ligand-binding molecules from this library in few weeks. There are, however, few studies in which the phage display technique has been used to create therapeutically useful structural variants of a bioactive protein, such as a mutein with stronger bioactivity and longer plasma half-life. To create a lysine-deficient mutant TNF-α, a phage library displaying mutant TNF-α lacking any lysine residue was prepared, and it consisted of $< 1 \times 10^8$ independent structural variants. After two rounds of biopanning against TNF-receptor, a lysine-deficient mutant TNF-α, mTNF-K90R, with an *in vitro* bioactivity that was 6-fold stronger than that of the wild-type TNF-α (wTNF-α) was obtained, despite reports that some of the lysine residues of TNF-α were essential for its bioactivity. This mTNF-K90R had < 10-fold higher *in vivo* antitumor potency and 1.3-fold lower *in vivo* toxicity compared to those of wTNF-α. Therefore, the therapeutic window of mTNF-K90R was extended by < 13-fold more than that of the wTNF-α. Whereas multiple PEG molecules

attached randomly to various sites of wTNF-α, only a single PEG molecule attached selectively to the N-terminus of mTNF-K90R. The site-specific mono-PEGylated mTNF-K90R (sp-PEG-mTNF-K90R) exhibited 60% specific activity of that of the mTNF-K90R, whereas the randomly mono-PEGylated wTNF-α (ran-PEG-wTNF-α) exhibited only 6% specific activity of that of the wTNF-α (Table. 1). Surprisingly, the sp-PEG-mTNF-K90R showed higher *in vitro* bioactivity than the wTNF-α. Thus, these results suggest that by using this site-specific PEGylation method, we have been able to circumvent the problems associated with the random PEGylation method. The sp-PEG-mTNF-K90R exhibited an antitumor potency that was 3-fold, > 30-fold, and > 30-fold higher than the antitumor potency exhibited by mTNF-K90R, wTNF-α and ran-PEG-wTNF-α, respectively. *In vivo* toxicity of sp-PEG-mTNF-K90R was < 1.5-fold, 2.0-fold, and 0.6-fold lower than the *in vivo* toxicity exhibited by mTNF-K90R, wTNF-α, and ran-PEG-wTNF-α, respectively. Thus, the therapeutic window of sp-PEG-mTNF-K90R expanded by > 5-fold, 60-fold, and 18-fold than the therapeutic window of mTNF-K90R, wTNF-α, and ran-PEG-wTNF-α, respectively. These results clearly demonstrate the advantages of creating muteins and developing methods for site-specific PEGylation to promote pharmacoproteomic-based protein-drug discovery and development.

Site-specific polymer-conjugation is possible even for a protein whose N-terminal region plays an essential role in activation by making use of the differences between the reaction patterns of α-Amino Groups and ε-Amino Groups, and this could be achieved by first creating a functional lysine-deficient mutant and then introducing a new lysine residue in an area that is not connected with activation.

Functionalized polymer carriers as DDS

In order to deliver a bioconjugated drug to the targeted tissue, the conjugate must demonstrate desirable pharmacokinetic characteristics, such as plasma clearance and tissue distribution. It is well known that the *in vivo* pharmacokinetics of polymer-conjugated drugs, such as bioactive proteins, could be markedly influenced by the properties (such as electric charge and hydrophilic/hydrophobic balance) of the polymeric carriers attached to the drug surface[37,38]. Any increase in the therapeutic effect of a drug bioconjugated with a polymeric modifier could be attributed to the pharmacokinetics of the bioconjugated drug. Therefore, prior to selecting a polymeric modifier for bioconjugation, it is very important to take into consideration the influence of physicochemical characteristics on the pharmacokinetics of the polymer. For example, we have demonstrated that for increased retention in blood, polyvinylpyrrolidone (PVP) is overwhelmingly superior to PEG as a polymer carrier [39].

These series of advances have also led us to successfully synthesize polyvinylpyrrolidone-co-dimethyl maleic anhydride (PVD), a renal-targeting polymer carrier with pH-sensitive controlled release capability [37,40]. PVD attaches to the amino group of a protein at pH ≥8 and these PVD-protein conjugates gradually releases the proteins at pH ≤ 7 (Figure 3). Since the diseased tissues (including tissues with inflammation, cancer, etc.) generally have lower pH levels than the healthy ones, this means that PVD as a drug/protein carrier would usually respond to pH levels and release the bound drug/protein, but only in the diseased tissues. Amazingly, 80% of PVD administered intravenously to mice accumulated in the kidney in only a few hours and 40% of PVD remained in the kidney for 4-days (Figure 3). The PVD was selectively taken up by the epithelial cells of the renal tubule. It neither showed any sign of cytotoxicity nor did it cause any tissue damage in the kidney or elsewhere even when administered at a high dose. In addition, the PVD conjugate of anti-inflammatory protein superoxide dismutase (SOD) was found to be highly stable *in vivo* and it accumulated at high levels in the kidney following an

Table 1 *In vitro* bioactivity of mono-PEGylated forms of TNF-αs

	EC50 (ng/ml) (% of remaining activity)
wTNF	0.17
mTNF-K90R	0.03
ran-PEG-wTNF	2.85 (6.0%)
sp-PEG-mTNF-K90R	0.05 (60.0%)

The specific activity of the mono-PEGylated forms of TNF-α was measured by a cytotoxic assay using LM cells in the presence of actinomycin D. EC_{50} is the concentration of various PEGylated TNF-αs capable of killing 50% of the cells.

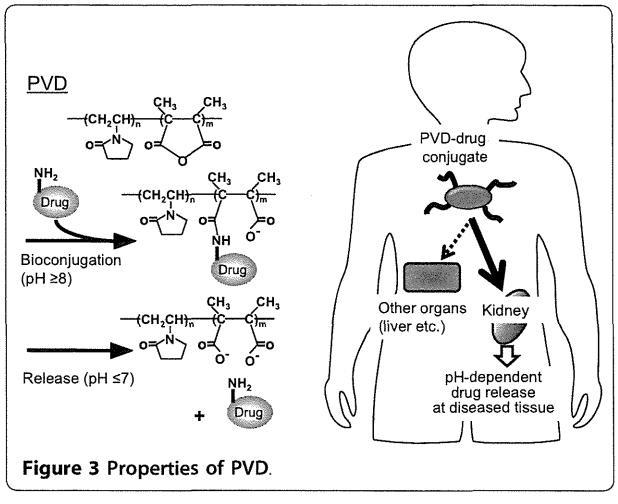

Figure 3 Properties of PVD.

intravenous injection, bringing out the possibility that this conjugate may have significant therapeutic value in treating kidney inflammation.

There is no cure for renal disease, which is a serious problem on the rise world-wide, and very few preventive strategies are available against this disease. Bioactive proteins, such as SOD and IL-10, were thought to be able to prevent the progression of renal disease, but their therapeutic potencies were too low because they were poorly distributed in the kidney. Many researchers have made attempts to deliver drug to the kidney. However, so far, there is no available report on delivery of drugs specifically to the kidney. Development of a renal delivery system that selectively carries drugs to the kidney is a promising way of limiting the tissue distribution of drugs and controlling the drug-associated toxicity. Therefore, PVD may be a new and useful renal-targeting drug carrier, and PVD-SOD conjugate may find clinical applications in the effective treatment of various renal diseases.

Conclusions

In this review, we have demonstrated the usefulness of DDS-based technologies to selectively enhance the desirable therapeutic activities of bioactive proteins without increasing their side effects. Thus, we suggest that, to further promote the clinical applications of bioactive proteins, it is necessary for the protein-drug innovation system to combine 1) a method for creating mutant proteins (muteins) with desired properties and 2) a bioconjugation method that generates conjugated products with optimal properties, such as targeting capability. We believe that this protein-drug innovation system will be a valuable tool for the development of novel protein-based therapies.

Acknowledgements

This study was supported in part by Grants-in-Aid for Scientific Research from the Ministry of Education, Culture, Sports, Science and Technology of Japan, and from the Japan Society for the Promotion of Science (JSPS). This study was also supported in part by Health Labour Sciences Research Grants from the Ministry of Health, Labor and Welfare of Japan; by Health Sciences Research Grants for Research on Publicly Essential Drugs and Medical Devices from the Japan Health Sciences Foundation; by a Global Environment Research Fund from Minister of the Environment; and by a the Knowledge Cluster Initiative; and by The Nagai Foundation Tokyo; and by The Takeda Science Foundation.

Author details

[1]Department of Toxicology and Safety Science, Graduate School of Pharmaceutical Sciences, Osaka University, 1-6 Yamadaoka, Suita, Osaka 565-0871, Japan. [2]The Center for Advanced Medical Engineering and Informatics, Osaka University, 1-6, Yamadaoka, Suita, Osaka 565-0871, Japan. [3]Laboratory of Biopharmaceutical Research, National Institute of Biomedical Innovation, 7-6-8, Saito-Asagi, Ibaraki, Osaka 567-0085, Japan. [4]Department of Biomedical Innovation, Graduate school of Pharmaceutical Sciences, Osaka University, 7-6-8 Saito-asagi, Ibaraki, Osaka 567-0085, Japan.

Authors' contributions

YY and ST wrote the manuscript. YT supervised the project. All authors discussed the results and commented on the manuscript.

Competing interests

The authors declare that they have no competing interests.

Received: 1 March 2011 Accepted: 12 May 2011 Published: 12 May 2011

References

1. Nishimoto N, Kishimoto T: **Interleukin 6: from bench to bedside.** *Nat Clin Pract Rheumatol* 2006, **2**:619-626.
2. Pastan I, Hassan R, FitzGerald DJ, Kreitman RJ: **Immunotoxin treatment of cancer.** *Annu Rev Med* 2007, **58**:221-237.
3. Szekanecz Z, Kerekes G, Soltesz P: **Vascular effects of biologic agents in RA and spondyloarthropathies.** *Nat Rev Rheumatol* 2009, **5**:677-684.
4. Aghemo A, Rumi MG, Colombo M: **Pegylated interferons alpha2a and alpha2b in the treatment of chronic hepatitis C.** *Nat Rev Gastroenterol Hepatol* 2010, **7**:485-494.
5. Kimura K, Taguchi T, Urushizaki I, Ohno R, Abe O, Furue H, Hattori T, Ichihashi H, Inoguchi K, Majima H, *et al*: **Phase I study of recombinant human tumor necrosis factor.** *Cancer Chemother Pharmacol* 1987, **20**:223-229.
6. Rosenberg SA, Lotze MT, Muul LM, Chang AE, Avis FP, Leitman S, Linehan WM, Robertson CN, Lee RE, Rubin JT, *et al*: **A progress report on the treatment of 157 patients with advanced cancer using lymphokine-activated killer cells and interleukin-2 or high-dose interleukin-2 alone.** *N Engl J Med* 1987, **316**:889-897.
7. Yoshioka Y, Tsutsumi Y, Nakagawa S, Mayumi T: **Recent progress on tumor missile therapy and tumor vascular targeting therapy as a new approach.** *Curr Vasc Pharmacol* 2004, **2**:259-270.
8. Pasut G, Veronese FM: **PEG conjugates in clinical development or use as anticancer agents: an overview.** *Adv Drug Deliv Rev* 2009, **61**:1177-1188.
9. Maeda H: **Tumor-selective delivery of macromolecular drugs via the EPR effect: background and future prospects.** *Bioconjug Chem* 2010, **21**:797-802.
10. Monkarsh SP, Ma Y, Aglione A, Bailon P, Ciolek D, DeBarbieri B, Graves MC, Hollfelder K, Michel H, Palleroni A, Porter JE, Russoman E, Roy S, Pan YC: **Positional isomers of monopegylated interferon alpha-2a: isolation, characterization, and biological activity.** *Anal Biochem* 1997, **247**:434-440.
11. Bailon P, Palleroni A, Schaffer CA, Spence CL, Fung WJ, Porter JE, Ehrlich GK, Pan W, Xu ZX, Modi MW, Farid A, Berthold W, Graves M: **Rational design of a potent, long-lasting form of interferon: a 40 kDa branched polyethylene glycol-conjugated interferon alpha-2a for the treatment of hepatitis C.** *Bioconjug Chem* 2001, **12**:195-202.
12. Carswell EA, Old LJ, Kassel RL, Green S, Fiore N, Williamson B: **An endotoxin-induced serum factor that causes necrosis of tumors.** *Proc Natl Acad Sci USA* 1975, **72**:3666-3670.
13. Blick M, Sherwin SA, Rosenblum M, Gutterman J: **Phase I study of recombinant tumor necrosis factor in cancer patients.** *Cancer Res* 1987, **47**:2986-2989.
14. Abbruzzese JL, Levin B, Ajani JA, Faintuch JS, Saks S, Patt YZ, Edwards C, Ende K, Gutterman JU: **Phase I trial of recombinant human gamma-interferon and recombinant human tumor necrosis factor in patients with advanced gastrointestinal cancer.** *Cancer Res* 1989, **49**:4057-4061.
15. Creaven PJ, Plager JE, Dupere S, Huben RP, Takita H, Mittelman A, Proefrock A: **Phase I clinical trial of recombinant human tumor necrosis factor.** *Cancer Chemother Pharmacol* 1987, **20**:137-144.
16. Chapman PB, Lester TJ, Casper ES, Gabrilove JL, Wong GY, Kempin SJ, Gold PJ, Welt S, Warren RS, Starnes HF, *et al*: **Clinical pharmacology of recombinant human tumor necrosis factor in patients with advanced cancer.** *J Clin Oncol* 1987, **5**:1942-1951.
17. Sherman ML, Spriggs DR, Arthur KA, Imamura K, Frei E, Kufe DW: **Recombinant human tumor necrosis factor administered as a five-day continuous infusion in cancer patients: phase I toxicity and effects on lipid metabolism.** *J Clin Oncol* 1988, **6**:344-350.
18. Tsutsumi Y, Kihira T, Yamamoto S, Kubo K, Nakagawa S, Miyake M, Horisawa Y, Kanamori T, Ikegami H, Mayumi T: **Chemical modification of natural human tumor necrosis factor-alpha with polyethylene glycol increases its anti-tumor potency.** *Jpn J Cancer Res* 1994, **85**:9-12.

19. Tsutsumi Y, Kihira T, Tsunoda S, Kubo K, Miyake M, Kanamori T, Nakagawa S, Mayumi T: **Intravenous administration of polyethylene glycol-modified tumor necrosis factor-alpha completely regressed solid tumor in Meth-A murine sarcoma model.** *Jpn J Cancer Res* 1994, **85**:1185-1188.
20. Tsutsumi Y, Kihira T, Tsunoda S, Kanamori T, Nakagawa S, Mayumi T: **Molecular design of hybrid tumour necrosis factor alpha with polyethylene glycol increases its anti-tumour potency.** *Br J Cancer* 1995, **71**:963-968.
21. Tsutsumi Y, Kihira T, Tsunoda S, Kamada H, Nakagawa S, Kaneda Y, Kanamori T, Mayumi T: **Molecular design of hybrid tumor necrosis factor-alpha III: polyethylene glycol-modified tumor necrosis factor-alpha has markedly enhanced antitumor potency due to longer plasma half-life and higher tumor accumulation.** *J Pharmacol Exp Ther* 1996, **278**:1006-1011.
22. Tsutsumi Y, Tsunoda S, Kamada H, Kihira T, Nakagawa S, Kaneda Y, Kanamori T, Mayumi T: **Molecular design of hybrid tumour necrosis factor-alpha. II: The molecular size of polyethylene glycol-modified tumour necrosis factor-alpha affects its anti-tumour potency.** *Br J Cancer* 1996, **74**:1090-1095.
23. Tsutsumi Y, Tsunoda S, Kaneda Y, Kamada H, Kihira T, Nakagawa S, Yamamoto Y, Horisawa Y, Mayumi T: **In vivo anti-tumor efficacy of polyethylene glycol-modified tumor necrosis factor-alpha against tumor necrosis factor-resistant tumors.** *Jpn J Cancer Res* 1996, **87**:1078-1085.
24. Hershfield MS: **PEG-ADA replacement therapy for adenosine deaminase deficiency: an update after 8.5 years.** *Clin Immunol Immunopathol* 1995, **76**:S228-232.
25. Chapes SK, Simske SJ, Sonnenfeld G, Miller ES, Zimmerman RJ: **Effects of spaceflight and PEG-IL-2 on rat physiological and immunological responses.** *J Appl Physiol* 1999, **86**:2065-2076.
26. Maeda H: **SMANCS and polymer-conjugated macromolecular drugs: advantages in cancer chemotherapy.** *Adv Drug Deliv Rev* 2001, **46**:169-185.
27. Talpaz M, O'Brien S, Rose E, Gupta S, Shan J, Cortes J, Giles FJ, Faderl S, Kantarjian HM: **Phase 1 study of polyethylene glycol formulation of interferon alpha-2B (Schering 54031) in Philadelphia chromosome-positive chronic myelogenous leukemia.** *Blood* 2001, **98**:1708-1713.
28. Isidori A, Tani M, Bonifazi F, Zinzani P, Curti A, Motta MR, Rizzi S, Giudice V, Farese O, Rovito M, Alinari L, Conte R, Baccarani M, Lemoli RM: **Phase II study of a single pegfilgrastim injection as an adjunct to chemotherapy to mobilize stem cells into the peripheral blood of pretreated lymphoma patients.** *Haematologica* 2005, **90**:225-231.
29. Jones EY, Stuart DI, Walker NP: **Structure of tumour necrosis factor.** *Nature* 1989, **338**:225-228.
30. Yamagishi J, Kawashima H, Matsuo N, Ohue M, Yamayoshi M, Fukui T, Kotani H, Furuta R, Nakano K, Yamada M: **Mutational analysis of structure–activity relationships in human tumor necrosis factor-alpha.** *Protein Eng* 1990, **3**:713-719.
31. Van Ostade X, Tavernier J, Prange T, Fiers W: **Localization of the active site of human tumour necrosis factor (hTNF) by mutational analysis.** *EMBO J* 1991, **10**:827-836.
32. Yamamoto Y, Tsutsumi Y, Yoshioka Y, Nishibata T, Kobayashi K, Okamoto T, Mukai Y, Shimizu T, Nakagawa S, Nagata S, Mayumi T: **Site-specific PEGylation of a lysine-deficient TNF-alpha with full bioactivity.** *Nat Biotechnol* 2003, **21**:546-552.
33. Shibata H, Yoshioka Y, Ikemizu S, Kobayashi K, Yamamoto Y, Mukai Y, Okamoto T, Taniai M, Kawamura M, Abe Y, Nakagawa S, Hayakawa T, Nagata S, Yamagata Y, Mayumi T, Kamada H, Tsutsumi Y: **Functionalization of tumor necrosis factor-alpha using phage display technique and PEGylation improves its antitumor therapeutic window.** *Clin Cancer Res* 2004, **10**:8293-8300.
34. Nielsen UB, Marks JD: **Internalizing antibodies and targeted cancer therapy: direct selection from phage display libraries.** *Pharm Sci Technolo Today* 2000, **3**:282-291.
35. Ruoslahti E: **Targeting tumor vasculature with homing peptides from phage display.** *Semin Cancer Biol* 2000, **10**:435-442.
36. Mukai Y, Yoshioka Y, Tsutsumi Y: **Phage display and PEGylation of therapeutic proteins.** *Comb Chem High Throughput Screen* 2005, **8**:145-152.
37. Kaneda Y, Tsutsumi Y, Yoshioka Y, Kamada H, Yamamoto Y, Kodaira H, Tsunoda S, Okamoto T, Mukai Y, Shibata H, Nakagawa S, Mayumi T: **The use of PVP as a polymeric carrier to improve the plasma half-life of drugs.** *Biomaterials* 2004, **25**:3259-3266.
38. Yoshioka Y, Tsutsumi Y, Ikemizu S, Yamamoto Y, Shibata H, Nishibata T, Mukai Y, Okamoto T, Taniai M, Kawamura M, Abe Y, Nakagawa S, Nagata S, Yamagata Y, Mayumi T: **Optimal site-specific PEGylation of mutant TNF-alpha improves its antitumor potency.** *Biochem Biophys Res Commun* 2004, **315**:808-814.
39. Kamada H, Tsutsumi Y, Yamamoto Y, Kihira T, Kaneda Y, Mu Y, Kodaira H, Tsunoda SI, Nakagawa S, Mayumi T: **Antitumor activity of tumor necrosis factor-alpha conjugated with polyvinylpyrrolidone on solid tumors in mice.** *Cancer Res* 2000, **60**:6416-6420.
40. Kamada H, Tsutsumi Y, Sato-Kamada K, Yamamoto Y, Yoshioka Y, Okamoto T, Nakagawa S, Nagata S, Mayumi T: **Synthesis of a poly (vinylpyrrolidone-co-dimethyl maleic anhydride) co-polymer and its application for renal drug targeting.** *Nat Biotechnol* 2003, **21**:399-404.

doi:10.1186/1752-153X-5-25
Cite this article as: Yoshioka *et al.*: Development of a novel DDS for site-specific PEGylated proteins. *Chemistry Central Journal* 2011 **5**:25.

ELSEVIER

Pathological changes in tight junctions and potential applications into therapies

Azusa Takahashi, Masuo Kondoh, Hidehiko Suzuki, Akihiro Watari and Kiyohito Yagi

Laboratory of Bio-Functional Molecular Chemistry, Graduate School of Pharmaceutical Sciences, Osaka University, Osaka 565-0871, Japan

Epithelial cells are pivotal in the separation of the body from the outside environment. Orally administered drugs must pass across epithelial cell sheets, and most pathological organisms invade the body through epithelial cells. Tight junctions (TJs) are sealing complexes between adjacent epithelial cells. Modulation of TJ components is a potent strategy for increasing absorption. Inflammation often causes disruption of the TJ barrier. Molecular imaging technology has enabled elucidation of the dynamics of TJs. Molecular pathological analysis has shown the relationship between TJ components and molecular pathological conditions. In this article, we discuss TJ-targeted drug development over the past 2 years.

During evolution from single-celled to multi-celled organisms, a compartment system developed to separate the inside of the body from the outside environment. This compartment system is made up of epithelial and endothelial cell sheets. Sealing of the intercellular space between individual epithelial or endothelial cells is crucial for compartmentalization.

Tight junctions (TJs) are the apical-most component of intercellular seals. TJs are directly involved both in the sealing of paracellular spaces and in two major functions of membranes: the barrier function and the fence function [1,2]. The barrier function is the first line of defense against pathogenic microorganisms and xenobiotics, and the fence function regulates cellular polarity. Deregulation of these functions is often observed in infectious diseases, inflammation and carcinogenesis.

Freeze-fracture electron microscopy analysis has shown that TJs are a set of continuous and anastomosing strands [3]. A series of analyses revealed that TJ-seals contain integral membrane proteins, such as occludin, claudins and junctional adhesion molecules (Fig. 1) [4–6]. The claudin protein family comprises 27 members and the junctional adhesion molecule (JAM) family comprises 3 members [4,7]. A tricellular junction-sealing component, tricellulin, has also been identified in epithelial cell sheets [8]. Occludin and tricellulin contain the tetra-spanning and other related proteins for vesicle trafficking and membrane line (MARVEL) domain. Occludin and tricellulin are members of the MARVEL protein family [9]. MarvelD3, another member of the MARVEL protein family, has been identified as a component of TJs [10]. The intracellular constituents of TJs, ZO-1 and ZO-2, determine where the claudin-based strands are formed [11]. Lipolysis-stimulated lipoprotein receptors define where tricellular junctions are formed [12]. These biochemical components of TJ-seals were all clarified within a single decade [5,6,13]. Our understanding of TJ-components has provided us with a new perspective on drug delivery and drug discovery for infectious diseases, inflammations and cancers [14–16].

There have been two main progressions in our understanding of the biology of TJs within the past 2 years: mucosal barrier homeostasis and TJ barrier homeostasis. Proof-of-concepts for TJ-targeted drug delivery have been demonstrated. In this article, we discuss recent topics in TJ biology and TJ-targeted therapy.

Biology of the epithelial barrier

Tight junctions

Epithelium is central to the construction of multicellular animals. More than 60% of the cell types in the vertebrate body are epithelial cells. Epithelia enclose and partition the animal body, line all of its surfaces and cavities, and create internal compartments. Epithelial cells are structurally polarized into a basal side that is anchored to other tissue, and an apical side that is

Corresponding author:. Kondoh, M. (masuo@phs.osaka-u.ac.jp)

1359-6446/06/$ - see front matter © 2012 Published by Elsevier Ltd. doi:10.1016/j.drudis.2012.02.014

Please cite this article in press as: A. Takahashi, et al., Pathological changes in tight junctions and potential applications into therapies, Drug Discov Today (2012), doi:10.1016/j.drudis.2012.02.014

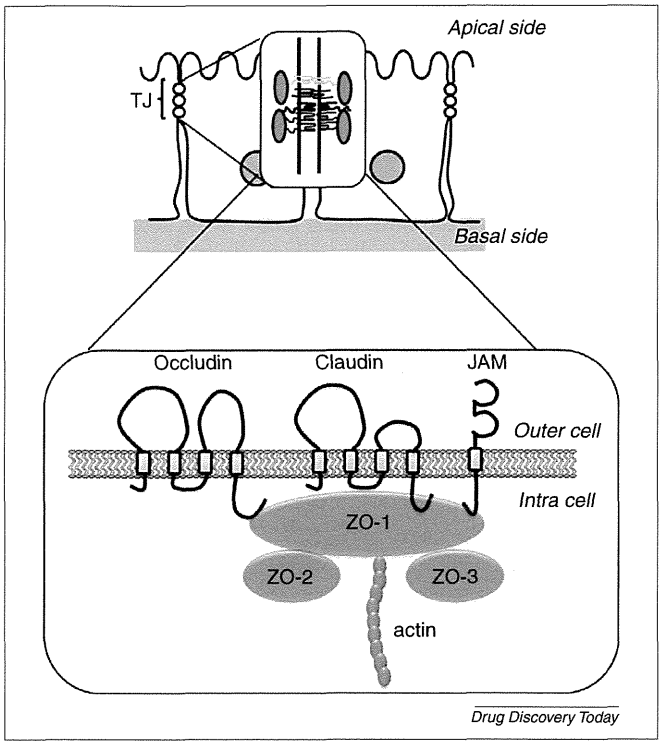

FIGURE 1

The epithelial barrier. Occludin, a tetra-transmembrane protein, was the first TJ-constituting protein identified [19]. Claudin was the second [21]. Claudins comprise a tetra-transmembrane protein family of 27 members. JAMs are glycosylated transmembrane proteins that belong to the immunoglobulin superfamily [4]. ZO-1, ZO-2 and ZO-3 are membrane-associated guanylate kinase proteins composed of a PSD95/Dlg/ZO-1 domain, an SH3 domain, a guanylate kinase domain, an acidic domain and an actin-binding region [68]. *Abbreviations*: JAMs: junctional adhesion molecules; TJ: tight junction;

unanchored. Adjacent epithelial cells are joined by occluding junctions called TJs. TJs have pivotal roles in separating the inside of the body from the outside environment, and in separating the inside and outside of tissues. TJs also function as a fence by preventing the free movement of apical membrane components and basal membrane components in epithelial cells.

TJs are intercellular sealing components located at the apical-most part of lateral membranes between adjacent epithelial cells and endothelial cells [17]. Adjacent TJ strands laterally associate with each other to form a paired strand thereby eliminating the intercellular space. Freeze fracture electron microscopy analysis revealed that TJs are continuous anastomosing intramembranous particle strands or fibrils with complementary grooves [3]. TJs are composed of transmembrane proteins, such as claudins, occludin and JAMs, in addition to cytoplasmic plaque proteins, including ZO-1, ZO-2, ZO-3 and cingulin [18].

Integral membrane proteins

Occludin was the first integral membrane protein identified in TJs [19]. Occludin has four transmembrane domains and has a molecular mass of approximately 65 kDa. Deletion of occludin does not affect the structure and function of TJs [20]. Claudins were the second integral membrane proteins identified in TJs [21]. Claudins comprise a multigene family with at least 27 members [7]. Claudins are 21–28-kDa proteins with tetratransmembrane domains. Claudins are key components in the structure and function of TJs [5,6]. A series of cellular analysis and knockout mouse analysis has clarified the roles of claudins in TJs [5,22].

Cytoplasmic proteins

ZO-1 was the first identified TJ-associated protein [23]. ZO-1, ZO-2 and ZO-3 contain PDZ-domains and the membrane-associated guanylate kinase domain. ZO-1, ZO-2 and ZO-3 are involved in formation of the TJ seal; they bind to the C-terminal cytoplasmic domain of occludin and claudins through the ZO PDZ domains [13]. ZO-1 and ZO-2 are crucial components for the definition of TJ formation [11].

Tricellular tight junctions

There are two types of TJs in epithelial cell sheets: bicellular and tricellular [2,24,25]. Occludin, claudins and JAMs are components of bicellular TJs. Tricellulin (approximately 65 kDa) is the only integral membrane component in tricellular TJs [8]. Tricellulin contains four transmembrane domains and shows structural similarity with occludin. Tricellulin is highly concentrated in tricellular TJs, but it is also localized in bicellular TJs [8,26]. Lipolysis-stimulated lipoprotein, a tricellular TJ-associated protein, defines tricellular contacts in epithelial cell sheets [12].

Mucosal barrier

The intestinal epithelium is where nutrients derived from food are absorbed, and it is also the first line of defense against microorganisms and xenobiotics. Regulation of the epithelial barrier is crucial for mucosal homeostasis. Recently, two intestinal epithelium proteins that regulate the intestinal barrier were identified.

The first protein is guanylyl cyclase C (GCC), which is a transmembrane receptor for the endogenous peptides guanylin and uroguanylin and for bacterial heat-stable enterotoxins [27]. GCC signaling has a pivotal role in the regulation of intestinal fluid and electrolyte homeostasis [28]. GCC-knockout mice show increased intestinal permeability, and GCC-knockdown in Caco-2 cells disrupts TJ integrity. This disruption of the TJ barrier is accompanied by phosphorylation of myosin II regulatory light chains, which induces TJ disassembly. GCC signaling is therefore involved in regulation of the TJ barrier [29].

The second intestinal membrane protein is matriptase. Matriptase is an integral membrane protein with trypsin-like serine protease activity and is a member of the type II transmembrane serine protease family [30]. It is widely expressed in all epithelia, and it is expressed in epithelial cells in the gastrointestinal tract [30]. Loss of matriptase reduces epithelial barrier integrity and enhances paracellular permeability. Matriptase facilitates claudin-2 loss from TJ complexes by indirect regulation of claudin-2 protein turnover by atypical protein kinase C zeta. Interestingly, matriptase does not affect some of the other TJ components, such as claudin-1, claudin-3, claudin-4, claudin-8, ZO-1, or E-cadherin [31].

These findings indicate that GCC signaling and matriptase might be potent targets for the treatment of intestinal disorders whose pathogenesis is disruption of the intestinal barrier function leading to mucosal inflammation and immune activation.

Please cite this article in press as: A. Takahashi, et al., Pathological changes in tight junctions and potential applications into therapies, Drug Discov Today (2012), doi:10.1016/j.drudis.2012.02.014